Supplemental Data

Impact of ^{18}F-FDG PET intensity normalization on radiomic features of oropharyngeal squamous cell carcinomas and machine learning–generated biomarkers

Table of Contents

1. Supplemental methods

1.1 PET voxel intensity value normalization

PET acquisition and reconstruction, including attenuation and decay corrections, were performed at the source institutions using standard clinical protocols. (a) In the absence of intensity normalization ("none", i.e., the "raw intensities"), PET voxel intensities usually represent the 18F-FDG activity concentration in Becquerels/milliliter. Whenever the image header indicated a different voxel value unit, we converted to Becquerels/milliliter. In addition, we generated three intensity-normalized images per patient: (b) body weight SUV-normalization was implemented following vender-neutral guidelines published by the FDG-PET/CT SUV Technical Subcommittee of the RSNA Quantitative Imaging Biomarkers Alliance (1). We also normalized PET images to reference tissues by taking the ratio of voxel intensities (i.e., standardized uptake ratio). The (c) left lentiform nucleus of the brain and the (d) cerebellum served as reference tissues (2-4). A detailed description of the measurement of reference tissue intensities is provided in sub-sections 1.1.1 and 1.1.2 below.

1.1.1 Measurement of PET voxel intensity values of left lentiform nucleus

All uptake corresponding to the left lentiform nucleus was manually segmented on axial PET slices to generate a three-dimensional volume of interest using the segment editor paint and erase tools in Slicer version 4.10.1 software (*5*). The right lentiform nucleus was used in case artifacts or brain pathologies obscured measurement of the left side. We used the segment statistics module in Slicer to determine the maximum voxel intensity value of the resulting volume of interest, which served as the reference uptake for intensity normalization.

1.1.2 Measurement of PET voxel intensity values of cerebellum

The cerebellum was segmented on a single axial slice using the co-registered computed tomography as guidance. To select an axial slice for segmentation, the *s* axial slices showing cerebellar tissue were counted, and the $(s/3)^{th}$ axial slice counted from caudal to cranial was selected. We included the cerebellar peduncles in the segmentation but excluded the fourth ventricle and brain stem. The segment editor level tracing tool in Slicer was used to create a crude segmentation of the cerebellum on the selected slice, which was manually refined using the paint and erase tools. Finally, the segment statistics module in Slicer calculated the mean voxel intensity value of the cerebellum segmentation, which served as the reference uptake for intensity normalization.

1.2 Tumor segmentation and radiomic feature extraction

Hypermetabolic areas on PET corresponding to the primary gross tumor volume were manually segmented slice-by-slice on the axial plane using 3D-Sliver version 4.10.1 software, as detailed previously (*4,5*). The resulting three-dimensional tumor mask and the corresponding PET images (four images resulting from four types of intensity normalization: "SUV", "none (raw intensities)", "lentiform nucleus", "cerebellum") were fed into a customized radiomics pipeline, which performed the image preprocessing and radiomics extraction. Only one tumor mask was generated per patient and used for feature extraction from all intensity-normalized image types.

Preprocessing included voxel dimension resampling by trilinear interpolation to an isotropic spacing of 3x3x3 mm and generation of derivative images by Laplacian of Gaussian (LoG) filtering with sigma settings of 3 mm and 6 mm generating n=2 derivative images as well as by performing a coif-1 wavelet transform with combinations of high- and low-pass filtering applied in each spatial direction generating n=8 additional derivate images (*6*). The extraction of some first-order features and certain texture feature families requires the discretization of voxel intensity values into bins as an additional preprocessing step (*6*). We used a fixed bin width method which is deemed more appropriate for PET (*6,7*). To obtain comparable radiomic feature values despite the variability in gray scale range, we adjusted the bin width for each combination of intensity normalization technique ("SUV", "none (raw intensities)", "lentiform nucleus", "cerebellum") and image type ("original", "LoG-filtered", "wavelet") to attain a median of n~80 bins per scan (see supplemental table 1, supplemental methods 3).

Subsequently, n=14 shape features were extracted from the original images, and n=18 first-order and n=75 texture features were extracted from the original and derived images (supplemental table 2) (*6*). This approach yielded n=1037 radiomic features per patient per PET intensity normalization technique. To perform the image preprocessing and radiomics extraction operations, a pyradiomics version 3.0.1 pipeline was configured with parameters reproduced in the supplemental methods 3 (*6,8*). Mathematical definitions of all pyradiomics features are included in the pyradiomics documentation (*6*) available from https://pyradiomics.readthedocs.io/_/downloads/en/v3.0.1/pdf/, all python source code is publicly accessible in the pyradiomics github (https://github.com/AIM-Harvard/pyradiomics/tree/master), and a user-friendly software version can be downloaded from https://pyradiomics.readthedocs.io/en/v3.0.1/.

1.3 Radiomics extraction parameters

1.3.1 Pyradiomics parameters for SUV-normalized PET

```
imageType:
  Original: {}
  LoG:
    sigma: [3.0, 6.0]
    binWidth: 0.0575
  Wavelet:
    binWidth: 0.0215

setting:
 resampledPixelSpacing: [3, 3, 3]
 interpolator: 'sitkLinear'
 padDistance: 10
 binWidth: 0.1165
```

1.3.2 Pyradiomics parameters for raw PET (no normalization)

```
imageType:
  Original: {}
  LoG:
    sigma: [3.0, 6.0]
    binWidth: 182
  Wavelet:
    binWidth: 72

setting:
 resampledPixelSpacing: [3, 3, 3]
 interpolator: 'sitkLinear'
 padDistance: 10
 binWidth: 363
```

1.3.3 Pyradiomics parameters for PET normalized to lentiform nucleus

```
imageType:
  Original: {}
  LoG:
    sigma: [3.0, 6.0]
    binWidth: 0.0056
  Wavelet:
    binWidth: 0.0021

setting:
 resampledPixelSpacing: [3, 3, 3]
 interpolator: 'sitkLinear'
 padDistance: 10
 binWidth: 0.0110
```

1.3.4 Pyradiomics parameters for PET normalized to cerebellum

```
imageType:
  Original: {}
  LoG:
    sigma: [3.0, 6.0]
    binWidth: 0.0088
  Wavelet:
    binWidth: 0.0033

setting:
 resampledPixelSpacing: [3, 3, 3]
 interpolator: 'sitkLinear'
 padDistance: 10
 binWidth: 0.0172
```

Radiomics extraction parameters were specified in parameter files written in YAML-convention as reproduced above. For details regarding specific parameters see reference (*6*).

LoG, Laplacian of Gaussian; PET, positron emission tomography; SUV, standardized uptake value.

1.4 Machine learning models for HPV prediction

To determine radiomic feature sets' utility in detecting HPV after PET intensity normalization, we devised, optimized, validated, and compared four separate machine learning models, each utilizing radiomic features from a different intensity-normalized image type. An XGBoost binary classifier ("xgb.train" function, "xgboost" package version 1.6.0.1 for R (*9*); function arguments: booster="gbtree", nrounds=300) combined with a MRMR filter feature selection algorithm ("mRMR.classic" function, "mRMRe" package version 2.0.9 for R (*10*)) formed the backbone of the machine learning pipeline. To devise and optimize models in the training cohort, we utilized 20 iterations of repeated stratified k-fold CV with k=5 and HPV-associated and -negative subpopulations as strata. Feature standardization, feature selection and XGBoost training were iteratively performed on the training folds to preclude information leakage to test folds. Models' performance was quantified in test folds and averaged across n=100 CV iterations (20x5-fold CV).

XGBoost hyperparameters were tuned in n=200 Bayesian optimization iterations ("BayesianOptimization" function, "rBayesianOptimization" package version 1.1.0 for R (*11*)); each hyperparameter set was evaluated in the 20x5-fold CV framework outlined above. Supplemental table 3 lists all optimized XGBoost parameters and their specified optimization range, with the remaining parameters kept at default recommendations. The MRMR algorithm ranked radiomic features and the number of top ranked radiomic features included in the models was also optimized as a hyperparameter (supplemental table 3). Subsequently, we performed MRMR feature selection and trained four final HPV classification models (one per each intensity-normalized image type) on the total training cohort using the optimized hyperparameters. Final models were validated in the independent and external validation cohorts. Feature importance scores for final models reflect features' "gain" as determined by the "xgb.importance" function ("xgboost" package version 1.6.0.1 for R (*9*)). This study employed a refined version of a machine learning pipeline reported previously (*4*).

2. Supplemental tables

Supplemental table 1 Bin widths and number of bins per patient obtained in image discretization

PET normalization method	Image	Bin width *	Number of bins per patient †		
			10th percentile	Median (IQR)	90th percentile
SUV	Original image	0.1165	26.1	80.0 (46.9-113.2)	149.7
	LoG-filtered images	0.0575	26.4	79.9 (48.5-120.5)	166.6
	Wavelet decompositions	0.0215	10.3	80.1 (26.8-243.4)	606.8
None (raw intensities)	Original image	363.0	26.3	80.0 (44.5-124.3)	187.6
	LoG-filtered images	182.0	26.5	80.1 (45.5-130.1)	193.3
	Wavelet decompositions	72.00	10.0	80.0 (25.7-237.3)	663.9
Reference tissue: lentiform nucleus	Original image	0.0110	27.5	80.4 (50.4-119.8)	164.9
	LoG-filtered images	0.0056	27.7	80.1 (49.3-119.5)	167.5
	Wavelet decompositions	0.0021	11.2	80.9 (27.5-241.2)	631.4
Reference tissue: cerebellum	Original image	0.0172	28.5	80.2 (52.1-118.4)	157.4
	LoG-filtered images	0.0088	29.2	79.8 (49.5-119.4)	164.6
	Wavelet decompositions	0.0033	11.2	80.3 (27.0-240.5)	638.7

* A fixed bin width image discretization method was applied as detailed in reference (*6*). The bin width setting was specified in pyradiomics parameter files which are reproduce in the supplemental methods 3.
† The resulting number of bins per patient was estimated based on the "Range" first-order feature value, and the bin width was adjusted to obtain a median number of n~80 bins per patient.

To obtain comparable radiomic feature values despite the variability in gray scale range, we adjusted the bin width for each combination of intensity normalization technique ("SUV", "none", "lentiform nucleus", "cerebellum") and image type ("original", "LoG-filtered", "wavelet") to attain a median of n~80 bins per patient.

IQR, interquartile range; LoG, Laplacian of Gaussian; PET, positron emission tomography; SUV, standardized uptake value.

Supplemental table 2 List of extracted radiomic features

Feature Family		Feature name	IBSI-compliance *
Shape	1	Elongation	YES
	2	Flatness	YES
	3	Least Axis Length	YES
	4	Major Axis Length	YES
	5	Maximum 2D Diameter (Column)	YES
	6	Maximum 2D Diameter (Row)	YES
	7	Maximum 2D Diameter (Slice)	YES
	8	Maximum 3D Diameter	YES
	9	Mesh Volume	NO §
	10	Minor Axis Length	YES
	11	Sphericity	YES
	12	Surface Area	YES
	13	Surface Area to Volume Ratio	YES
	14	Voxel Volume	NO §
First-order	1	10th percentile	YES
	2	90th percentile	YES
	3	Energy	YES
	4	Entropy	NO §
	5	Interquartile Range	YES
	6	Kurtosis	NO †
	7	Maximum	YES
	8	Mean	YES
	9	Mean Absolute Deviation	YES
	10	Median	YES
	11	Minimum	YES
	12	Range	YES
	13	Robust Mean Absolute Deviation	YES
	14	Root Mean Squared	YES
	15	Skewness	YES
	16	Total Energy	NO ‡
	17	Uniformity	NO §
	18	Variance	YES
Texture - Gray Level Cooccurrence Matrix Features (GLCM)	1	Autocorrelation	YES
	2	Cluster Prominence	YES
	3	Cluster Shade	YES
	4	Cluster Tendency	YES
	5	Contrast	YES
	6	Correlation	YES
	7	Difference Average	YES
	8	Difference Entropy	YES
	9	Difference Variance	YES
	10	Informational Measure of Correlation 1	YES
	11	Informational Measure of Correlation 2	YES

	12	Inverse Difference	YES
	13	Inverse Difference Moment	YES
	14	Inverse Difference Moment Normalized	YES
	15	Inverse Difference Normalized	YES
	16	Inverse Variance	YES
	17	Joint Average	YES
	18	Joint Energy	NO [§]
	19	Joint Entropy	YES
	20	Maximal Correlation Coefficient	YES
	21	Maximum Probability	NO [§]
	22	Sum Average	YES
	23	Sum Entropy	YES
	24	Sum of Squares	NO [§]
Texture - Gray Level Size Zone Matrix Features (GLSZM)	1	Gray Level Non-Uniformity	YES
	2	Gray Level Non-Uniformity Normalized	YES
	3	Gray Level Variance	YES
	4	High Gray Level Zone Emphasis	YES
	5	Large Area Emphasis	YES
	6	Large Area High Gray Level Emphasis	YES
	7	Large Area Low Gray Level Emphasis	YES
	8	Low Gray Level Zone Emphasis	YES
	9	Size Zone Non-Uniformity	YES
	10	Size Zone Non-Uniformity Normalized	YES
	11	Small Area Emphasis	YES
	12	Small Area High Gray Level Emphasis	YES
	13	Small Area Low Gray Level Emphasis	YES
	14	Zone Entropy	YES
	15	Zone Percentage	YES
	16	Zone Variance	YES
Texture - Gray Level Run Length Matrix Features (GLRLM)	1	Gray Level Non-Uniformity	YES
	2	Gray Level Non-Uniformity Normalized	YES
	3	Gray Level Variance	YES
	4	High Gray Level Run Emphasis	YES
	5	Long Run Emphasis	YES
	6	Long Run High Gray Level Emphasis	YES
	7	Long Run Low Gray Level Emphasis	YES
	8	Low Gray Level Run Emphasis	YES
	9	Run Entropy	YES
	10	Run Length Non Uniformity	YES
	11	Run Length Non Uniformity Normalized	YES
	12	Run Percentage	YES
	13	Run Variance	YES
	14	Short Run Emphasis	YES

	15	Short Run High Gray Level Emphasis	YES
	16	Short Run Low Gray Level Emphasis	YES
Texture - Neighboring Gray Tone Difference Matrix Features (NGTDM)	1	Busyness	YES
	2	Coarseness	YES
	3	Complexity	YES
	4	Contrast	YES
	5	Strength	YES
Texture - Gray Level Dependence Matrix Features (GLDM)	1	Dependence Entropy	YES
	2	Dependence Non-Uniformity	YES
	3	Dependence Non-Uniformity Normalized	YES
	4	Dependence Variance	YES
	5	Gray Level Non-Uniformity	YES
	6	Gray Level Variance	YES
	7	High Gray Level Emphasis	YES
	8	Large Dependence Emphasis	YES
	9	Large Dependence High Gray Level Emphasis	YES
	10	Large Dependence Low Gray Level Emphasis	YES
	11	Low Gray Level Emphasis	YES
	12	Small Dependence Emphasis	YES
	13	Small Dependence High Gray Level Emphasis	YES
	14	Small Dependence Low Gray Level Emphasis	YES

* Indicates if the pyradiomics feature definition including the feature name complies with the image biomarker standardization initiative (IBSI)-definition (*12*). Reference (*6*) provides exact pyradiomcs feature definitions including a documentation of the differences.
† IBSI-compliant after feature standardization.
‡ Not defined by IBSI.
§ Mathematically identical to IBSI definition; different naming only.

Complete list of pyradiomics features used in this study. Exact feature definitions are provided in reference (*6*).

IBSI, image biomarker standardization initiative.

Supplemental table 3 Bayesian optimization of XGBoost parameters

Hyperparameter *	Lower parameter bound	Upper parameter bound
Number of radiomic features †	2	30
eta	0	1
gamma	0	10
max_depth	3	15
min_child_weight	0	20
subsample	0.4	1
colsample_bytree	0.4	1
lambda	0.5	1

* For parameter definitions, refer to ref. (*9*).
† The MRMR algorithm ranked radiomic features. From the top of this list, the *n* most valuable radiomic features were included in the XGBoost model. Bayesian optimization was used to optimize *n*.

Bayesian optimization was utilized to tune XGBoost hyperparameters. The table lists all optimized XGBoost parameters including the upper and lower bounds of the optimization range. We set the remaining parameters to the default recommendations.

MRMR, minimum redundancy maximum relevance feature selection; XGBoost, extreme gradient boosting machine learning classifier.

Supplemental table 4 Patients' characteristics

	Training cohort	Independent validation cohort	External validation cohort (MAASTRO)	p-value			HPV associated cancers	HPV negative cancers	Total cohort
				training vs. indep.	training vs. external	indep. vs. external			
Number of patients	325	79	26				313	117	430
Sex – n (%)									
male	271 (83.4 %)	64 (81.0 %)	22 (84.6 %)	0.62	0.87	0.68	261 (83,4 %)	96 (82.1 %)	357 (83.0 %)
female	54 (16.6 %)	15 (19.0 %)	4 (15.4 %)				52 (16.6 %)	21 (17.9 %)	73 (17.0 %)
Age [years] – mean (SD)	60.63 (9.30)	60.27 (8.81)	61.19 (7.30)	0.62	0.65	0.46	60.23 (8.64)	61.58 (10.17)	60.60 (9.09)
HPV status * – n (%)									
positive	244 (75.1 %)	59 (74.7 %)	10 (38.5 %)	0.94	<0.0001*	0.0007*	313 (100 %)	0 (0 %)	313 (72.8 %)
negative	81 (24.9 %)	20 (25.3 %)	16 (61.5 %)				0 (0 %)	117 (100 %)	117 (27.2 %)
T stage † – n (%)									
T1	46 (14.2 %)	6 (7.6 %)	4 (15.4 %)	0.32	0.94	0.70	44 (14.1 %)	12 (10.3 %)	56 (13.0 %)
T2	120 (36.9 %)	35 (44.3 %)	10 (38.5 %)				131 41.9 %)	34 (29.1 %)	165 (38.4 %)
T3	106 (32.6 %)	23 (29.1 %)	7 (26.9 %)				98 (31.1 %)	38 (32.5 %)	136 (31.6 %)
T4	53 (16.3 %)	15 (19.0 %)	5 (19.2 %)				40 (12.8 %)	33 (28.2 %)	73 (17.0 %)
N stage † – n (%)									
N0	63 (19.4 %)	14 (17.7 %)	4 (15.4 %)	0.71	0.39	0.31	56 (17.9 %)	25 (21.4 %)	81 (18.8 %)
N1	143 (44.0 %)	40 (50.6 %)	9 (34.6 %)				171 (54.6 %)	21 (17.9 %)	192 (44.7 %)
N2	111 (34.2 %)	24 (30.4 %)	13 (50.0 %)				80 (25.6 %)	68 (58.1 %)	148 (34.4 %)
N3	8 (2.5 %)	1 (1.3 %)	0 (0.0 %)				6 (1.9 %)	3 (2.6 %)	9 (2.1 %)
M stage † – n (%)									
M0	311 (95.7%)	77 (97.5 %)	26 (100.0 %)	0.47	0.28	0.41	307 (98.1 %)	107 (91.5 %)	414 (96.3 %)
M1	14 (4.3 %)	2 (2.5 %)	0 (0.0 %)				6 (1.9 %)	10 (8.5 %)	16 (3.7 %)
Overall stage *, † – n (%)									
I	110 (33.8 %)	31 (39.2 %)	6 (23.1 %)	0.82	0.04 *	0.10 *	143 (45.7 %)	4 (3.4 %)	147 (34.2 %)
II	100 (30.8 %)	22 (27.8 %)	5 (19.2 %)				118 (37.7 %)	9 (7.7 %)	127 (29.5 %)
III	53 (16.3 %)	11 (13.9 %)	4 (15.4 %)				46 (14.7 %)	22 (18.8 %)	68 (15.8 %)
IV	62 (19.1 %)	15 (19.0 %)	11 (42.3 %)				6 (1.9 %)	82 (70.1 %)	88 (20.5 %)
PET ‡ – mean (SD)									
slice thickness [mm]	3.37 (0.37)	3.33 (0.43)	3 §	0.63	n.a.§	n.a.§	3.34 (0.40)	3.34 (0.33)	3.34 (0.38)
in-plane voxel spacing [mm]	4.33 (0.92)	4.35 (0.93)	2.67 §	0.74	n.a.§	n.a.§	4.25 (0.96)	4.19 (1.02)	4.23 (0.97)
in-plane image matrix [n x n]	149.39 (58.86) x idem	155.14 (67.90) x idem	256 x 256 §	0.49	n.a.§	n.a.§	156.42 (66.34) x idem	158.15 (57.43) x idem	156.89 (63.98) x idem

* The external validation cohort had a higher proportion of HPV-negative cancers, leading to a higher proportion of late-stage patients, compared to the training and independent validation cohorts.
† TNM / overall stage per AJCC 8th edition staging manual.
‡ Values are from original images before pre-processing.
§ Identical imaging characteristics in entire external validation dataset.

HPV, human papilloma virus; indep., independent; n.a., not applicable; PET, positron emission tomography.

Supplemental table 5 ICC values of all radiomic features

Feature identifier *				
Pre-processing		Family	Feature name	ICC (95% CI)
Original	n/a	Shape	Elongation	1 (1 - 1)
Original	n/a	Shape	Flatness	1 (1 - 1)
Original	n/a	Shape	Least axis length	1 (1 - 1)
Original	n/a	Shape	Major axis length	1 (1 - 1)
Original	n/a	Shape	Maximum 2D diameter column	1 (1 - 1)
Original	n/a	Shape	Maximum 2D diameter row	1 (1 - 1)
Original	n/a	Shape	Maximum 2D diameter slice	1 (1 - 1)
Original	n/a	Shape	Maximum 3D diameter	1 (1 - 1)
Original	n/a	Shape	Mesh volume	1 (1 - 1)
Original	n/a	Shape	Minor axis length	1 (1 - 1)
Original	n/a	Shape	Sphericity	1 (1 - 1)
Original	n/a	Shape	Surface area	1 (1 - 1)
Original	n/a	Shape	Surface volume ratio	1 (1 - 1)
Original	n/a	Shape	Voxel volume	1 (1 - 1)
Original	n/a	First-order	10th percentile	0.494 (0.446 - 0.542)
Original	n/a	First-order	90th percentile	0.784 (0.755 - 0.811)
Original	n/a	First-order	Energy	0.904 (0.89 - 0.917)
Original	n/a	First-order	Entropy	0.921 (0.909 - 0.932)
Original	n/a	First-order	Interquartile range	0.887 (0.87 - 0.902)
Original	n/a	First-order	Kurtosis	1 (1 - 1)
Original	n/a	First-order	Maximum	0.797 (0.77 - 0.823)
Original	n/a	First-order	Mean absolute deviation	0.876 (0.858 - 0.892)
Original	n/a	First-order	Mean	0.705 (0.669 - 0.74)
Original	n/a	First-order	Median	0.699 (0.662 - 0.734)
Original	n/a	First-order	Minimum	0.444 (0.395 - 0.495)
Original	n/a	First-order	Range	0.858 (0.837 - 0.877)
Original	n/a	First-order	Robust mean absolute deviation	0.884 (0.867 - 0.899)
Original	n/a	First-order	Root mean squared	0.731 (0.697 - 0.763)
Original	n/a	First-order	Skewness	1 (1 - 1)
Original	n/a	First-order	Total energy	0.904 (0.89 - 0.917)
Original	n/a	First-order	Uniformity	0.904 (0.89 - 0.917)
Original	n/a	First-order	Variance	0.822 (0.797 - 0.845)
Original	n/a	GLCM	Autocorrelation	0.808 (0.782 - 0.832)
Original	n/a	GLCM	Cluster prominence	0.698 (0.661 - 0.733)
Original	n/a	GLCM	Cluster shade	0.776 (0.747 - 0.804)
Original	n/a	GLCM	Cluster tendency	0.829 (0.805 - 0.851)
Original	n/a	GLCM	Contrast	0.772 (0.742 - 0.8)
Original	n/a	GLCM	Correlation	1 (1 - 1)
Original	n/a	GLCM	Difference average	0.827 (0.803 - 0.85)
Original	n/a	GLCM	Difference entropy	0.903 (0.888 - 0.916)
Original	n/a	GLCM	Difference variance	0.782 (0.753 - 0.809)
Original	n/a	GLCM	Inverse difference	0.875 (0.857 - 0.892)
Original	n/a	GLCM	Inverse difference moment	0.873 (0.855 - 0.89)
Original	n/a	GLCM	Inverse difference moment normalized	0.996 (0.995 - 0.996)
Original	n/a	GLCM	Inverse difference normalized	0.997 (0.996 - 0.997)
Original	n/a	GLCM	Informational measure of correlation 1	0.864 (0.844 - 0.882)
Original	n/a	GLCM	Informational measure of correlation 2	0.758 (0.727 - 0.788)
Original	n/a	GLCM	Inverse variance	0.878 (0.86 - 0.895)
Original	n/a	GLCM	Joint average	0.854 (0.834 - 0.874)
Original	n/a	GLCM	Joint energy	0.957 (0.95 - 0.963)
Original	n/a	GLCM	Joint entropy	0.988 (0.986 - 0.99)
Original	n/a	GLCM	Maximal correlation coefficient	0.865 (0.845 - 0.883)
Original	n/a	GLCM	Maximum probability	0.921 (0.908 - 0.932)
Original	n/a	GLCM	Sum average	0.854 (0.834 - 0.874)
Original	n/a	GLCM	Sum entropy	0.96 (0.953 - 0.966)
Original	n/a	GLCM	Sum squares	0.82 (0.795 - 0.843)
Original	n/a	GLDM	Dependence entropy	0.981 (0.978 - 0.984)
Original	n/a	GLDM	Dependence non uniformity	0.982 (0.979 - 0.985)
Original	n/a	GLDM	Dependence non uniformity normalized	0.814 (0.788 - 0.838)
Original	n/a	GLDM	Dependence variance	0.718 (0.683 - 0.752)
Original	n/a	GLDM	Gray level non uniformity	0.938 (0.928 - 0.946)
Original	n/a	GLDM	Gray level variance	0.822 (0.797 - 0.845)
Original	n/a	GLDM	High gray level emphasis	0.81 (0.784 - 0.835)
Original	n/a	GLDM	Large dependence emphasis	0.757 (0.726 - 0.787)
Original	n/a	GLDM	Large dependence high gray level emphasis	0.9 (0.885 - 0.914)
Original	n/a	GLDM	Large dependence low gray level emphasis	0.599 (0.555 - 0.642)
Original	n/a	GLDM	Low gray level emphasis	0.86 (0.84 - 0.879)
Original	n/a	GLDM	Small dependence emphasis	0.828 (0.804 - 0.851)
Original	n/a	GLDM	Small dependence high gray level emphasis	0.786 (0.757 - 0.813)
Original	n/a	GLDM	Small dependence low gray level emphasis	0.939 (0.93 - 0.948)
Original	n/a	GLRLM	Gray level non uniformity	0.942 (0.933 - 0.95)
Original	n/a	GLRLM	Gray level non uniformity normalized	0.905 (0.891 - 0.918)
Original	n/a	GLRLM	Gray level variance	0.821 (0.797 - 0.844)
Original	n/a	GLRLM	High gray level run emphasis	0.81 (0.784 - 0.834)
Original	n/a	GLRLM	Long run emphasis	0.795 (0.767 - 0.82)
Original	n/a	GLRLM	Long run high gray level emphasis	0.815 (0.79 - 0.839)
Original	n/a	GLRLM	Long run low gray level emphasis	0.824 (0.8 - 0.847)
Original	n/a	GLRLM	Low gray level run emphasis	0.859 (0.839 - 0.878)
Original	n/a	GLRLM	Run entropy	0.93 (0.919 - 0.94)
Original	n/a	GLRLM	Run length non uniformity	0.999 (0.999 - 0.999)
Original	n/a	GLRLM	Run length non uniformity normalized	0.818 (0.792 - 0.841)
Original	n/a	GLRLM	Run percentage	0.813 (0.787 - 0.837)
Original	n/a	GLRLM	Run variance	0.787 (0.758 - 0.814)
Original	n/a	GLRLM	Short run emphasis	0.812 (0.786 - 0.836)
Original	n/a	GLRLM	Short run high gray level emphasis	0.809 (0.782 - 0.833)
Original	n/a	GLRLM	Short run low gray level emphasis	0.866 (0.847 - 0.884)
Original	n/a	GLSZM	Gray level non uniformity	0.967 (0.962 - 0.972)
Original	n/a	GLSZM	Gray level non uniformity normalized	0.892 (0.876 - 0.907)
Original	n/a	GLSZM	Gray level variance	0.816 (0.791 - 0.84)
Original	n/a	GLSZM	High gray level zone emphasis	0.805 (0.779 - 0.83)
Original	n/a	GLSZM	Large area emphasis	0.624 (0.582 - 0.665)
Original	n/a	GLSZM	Large area high gray level emphasis	0.887 (0.87 - 0.902)
Original	n/a	GLSZM	Large area low gray level emphasis	0.517 (0.469 - 0.564)
Original	n/a	GLSZM	Low gray level zone emphasis	0.814 (0.789 - 0.838)
Original	n/a	GLSZM	Size zone non uniformity	0.973 (0.969 - 0.977)
Original	n/a	GLSZM	Size zone non uniformity normalized	0.82 (0.795 - 0.843)
Original	n/a	GLSZM	Small area emphasis	0.819 (0.794 - 0.843)
Original	n/a	GLSZM	Small area high gray level emphasis	0.795 (0.767 - 0.821)

Feature identifier *				
Pre-processing		Family	Feature name	ICC (95% CI)
Original	n/a	GLSZM	Small area low gray level emphasis	0.837 (0.814 - 0.858)
Original	n/a	GLSZM	Zone entropy	0.968 (0.963 - 0.972)
Original	n/a	GLSZM	Zone percentage	0.825 (0.8 - 0.847)
Original	n/a	GLSZM	Zone variance	0.59 (0.546 - 0.634)
Original	n/a	NGTDM	Busyness	0.715 (0.679 - 0.749)
Original	n/a	NGTDM	Coarseness	0.987 (0.985 - 0.989)
Original	n/a	NGTDM	Complexity	0.761 (0.73 - 0.79)
Original	n/a	NGTDM	Contrast	0.756 (0.724 - 0.786)
Original	n/a	NGTDM	Strength	0.785 (0.756 - 0.812)
LoG	3 mm	First-order	10th percentile	0.787 (0.758 - 0.814)
LoG	3 mm	First-order	90th percentile	0.959 (0.953 - 0.965)
LoG	3 mm	First-order	Energy	0.861 (0.841 - 0.88)
LoG	3 mm	First-order	Entropy	0.894 (0.878 - 0.908)
LoG	3 mm	First-order	Interquartile range	0.846 (0.824 - 0.866)
LoG	3 mm	First-order	Kurtosis	1 (1 - 1)
LoG	3 mm	First-order	Maximum	0.936 (0.926 - 0.945)
LoG	3 mm	First-order	Mean absolute deviation	0.838 (0.815 - 0.859)
LoG	3 mm	First-order	Mean	0.774 (0.744 - 0.802)
LoG	3 mm	First-order	Median	0.814 (0.788 - 0.838)
LoG	3 mm	First-order	Minimum	0.817 (0.791 - 0.84)
LoG	3 mm	First-order	Range	0.847 (0.825 - 0.867)
LoG	3 mm	First-order	Robust mean absolute deviation	0.844 (0.822 - 0.864)
LoG	3 mm	First-order	Root mean squared	0.772 (0.742 - 0.8)
LoG	3 mm	First-order	Skewness	1 (1 - 1)
LoG	3 mm	First-order	Total energy	0.861 (0.841 - 0.88)
LoG	3 mm	First-order	Uniformity	0.878 (0.86 - 0.895)
LoG	3 mm	First-order	Variance	0.782 (0.753 - 0.809)
LoG	3 mm	GLCM	Autocorrelation	0.806 (0.779 - 0.831)
LoG	3 mm	GLCM	Cluster prominence	0.639 (0.598 - 0.679)
LoG	3 mm	GLCM	Cluster shade	0.737 (0.703 - 0.769)
LoG	3 mm	GLCM	Cluster tendency	0.79 (0.761 - 0.816)
LoG	3 mm	GLCM	Contrast	0.764 (0.733 - 0.793)
LoG	3 mm	GLCM	Correlation	1 (1 - 1)
LoG	3 mm	GLCM	Difference average	0.82 (0.795 - 0.843)
LoG	3 mm	GLCM	Difference entropy	0.885 (0.868 - 0.901)
LoG	3 mm	GLCM	Difference variance	0.77 (0.74 - 0.799)
LoG	3 mm	GLCM	Inverse difference	0.857 (0.836 - 0.875)
LoG	3 mm	GLCM	Inverse difference moment	0.852 (0.831 - 0.871)
LoG	3 mm	GLCM	Inverse difference moment normalized	0.997 (0.996 - 0.997)
LoG	3 mm	GLCM	Inverse difference normalized	0.998 (0.997 - 0.998)
LoG	3 mm	GLCM	Informational measure of correlation 1	0.906 (0.892 - 0.919)
LoG	3 mm	GLCM	Informational measure of correlation 2	0.797 (0.77 - 0.823)
LoG	3 mm	GLCM	Inverse variance	0.852 (0.831 - 0.872)
LoG	3 mm	GLCM	Joint average	0.86 (0.84 - 0.879)
LoG	3 mm	GLCM	Joint energy	0.948 (0.94 - 0.955)
LoG	3 mm	GLCM	Joint entropy	0.981 (0.978 - 0.984)
LoG	3 mm	GLCM	Maximal correlation coefficient	0.905 (0.89 - 0.918)
LoG	3 mm	GLCM	Maximum probability	0.936 (0.926 - 0.945)
LoG	3 mm	GLCM	Sum average	0.86 (0.84 - 0.879)
LoG	3 mm	GLCM	Sum entropy	0.943 (0.934 - 0.951)
LoG	3 mm	GLCM	Sum squares	0.783 (0.754 - 0.81)
LoG	3 mm	GLDM	Dependence entropy	0.978 (0.975 - 0.982)
LoG	3 mm	GLDM	Dependence non uniformity	0.979 (0.976 - 0.982)
LoG	3 mm	GLDM	Dependence non uniformity normalized	0.824 (0.8 - 0.847)
LoG	3 mm	GLDM	Dependence variance	0.806 (0.779 - 0.83)
LoG	3 mm	GLDM	Gray level non uniformity	0.943 (0.935 - 0.951)
LoG	3 mm	GLDM	Gray level variance	0.782 (0.753 - 0.809)
LoG	3 mm	GLDM	High gray level emphasis	0.801 (0.774 - 0.826)
LoG	3 mm	GLDM	Large dependence emphasis	0.781 (0.752 - 0.808)
LoG	3 mm	GLDM	Large dependence high gray level emphasis	0.877 (0.859 - 0.894)
LoG	3 mm	GLDM	Large dependence low gray level emphasis	0.613 (0.57 - 0.655)
LoG	3 mm	GLDM	Low gray level emphasis	0.901 (0.887 - 0.915)
LoG	3 mm	GLDM	Small dependence emphasis	0.82 (0.796 - 0.844)
LoG	3 mm	GLDM	Small dependence high gray level emphasis	0.781 (0.751 - 0.808)
LoG	3 mm	GLDM	Small dependence low gray level emphasis	0.973 (0.969 - 0.977)
LoG	3 mm	GLRLM	Gray level non uniformity	0.949 (0.941 - 0.956)
LoG	3 mm	GLRLM	Gray level non uniformity normalized	0.879 (0.861 - 0.895)
LoG	3 mm	GLRLM	Gray level variance	0.782 (0.753 - 0.809)
LoG	3 mm	GLRLM	High gray level run emphasis	0.801 (0.774 - 0.826)
LoG	3 mm	GLRLM	Long run emphasis	0.791 (0.762 - 0.817)
LoG	3 mm	GLRLM	Long run high gray level emphasis	0.805 (0.778 - 0.83)
LoG	3 mm	GLRLM	Long run low gray level emphasis	0.847 (0.826 - 0.867)
LoG	3 mm	GLRLM	Low gray level run emphasis	0.905 (0.891 - 0.918)
LoG	3 mm	GLRLM	Run entropy	0.907 (0.893 - 0.92)
LoG	3 mm	GLRLM	Run length non uniformity	0.999 (0.999 - 0.999)
LoG	3 mm	GLRLM	Run length non uniformity normalized	0.811 (0.785 - 0.835)
LoG	3 mm	GLRLM	Run percentage	0.807 (0.781 - 0.832)
LoG	3 mm	GLRLM	Run variance	0.788 (0.759 - 0.814)
LoG	3 mm	GLRLM	Short run emphasis	0.805 (0.778 - 0.83)
LoG	3 mm	GLRLM	Short run high gray level emphasis	0.8 (0.773 - 0.825)
LoG	3 mm	GLRLM	Short run low gray level emphasis	0.918 (0.905 - 0.929)
LoG	3 mm	GLSZM	Gray level non uniformity	0.981 (0.978 - 0.983)
LoG	3 mm	GLSZM	Gray level non uniformity normalized	0.876 (0.858 - 0.892)
LoG	3 mm	GLSZM	Gray level variance	0.781 (0.752 - 0.808)
LoG	3 mm	GLSZM	High gray level zone emphasis	0.799 (0.772 - 0.824)
LoG	3 mm	GLSZM	Large area emphasis	0.574 (0.528 - 0.618)
LoG	3 mm	GLSZM	Large area high gray level emphasis	0.85 (0.829 - 0.87)
LoG	3 mm	GLSZM	Large area low gray level emphasis	0.602 (0.559 - 0.645)
LoG	3 mm	GLSZM	Low gray level zone emphasis	0.92 (0.907 - 0.931)
LoG	3 mm	GLSZM	Size zone non uniformity	0.962 (0.956 - 0.967)
LoG	3 mm	GLSZM	Size zone non uniformity normalized	0.808 (0.782 - 0.833)
LoG	3 mm	GLSZM	Small area emphasis	0.798 (0.771 - 0.824)
LoG	3 mm	GLSZM	Small area high gray level emphasis	0.789 (0.761 - 0.816)
LoG	3 mm	GLSZM	Small area low gray level emphasis	0.902 (0.888 - 0.916)
LoG	3 mm	GLSZM	Zone entropy	0.963 (0.958 - 0.969)
LoG	3 mm	GLSZM	Zone percentage	0.817 (0.792 - 0.841)
LoG	3 mm	GLSZM	Zone variance	0.558 (0.512 - 0.603)
LoG	3 mm	NGTDM	Busyness	0.77 (0.739 - 0.798)

Feature identifier *				
Pre-processing		Family	Feature name	ICC (95% CI)
LoG	3 mm	NGTDM	Coarseness	0.989 (0.987 - 0.99)
LoG	3 mm	NGTDM	Complexity	0.753 (0.721 - 0.783)
LoG	3 mm	NGTDM	Contrast	0.758 (0.726 - 0.787)
LoG	3 mm	NGTDM	Strength	0.793 (0.765 - 0.819)
LoG	6 mm	First-order	10th percentile	0.814 (0.788 - 0.837)
LoG	6 mm	First-order	90th percentile	0.879 (0.862 - 0.896)
LoG	6 mm	First-order	Energy	0.868 (0.849 - 0.886)
LoG	6 mm	First-order	Entropy	0.928 (0.917 - 0.938)
LoG	6 mm	First-order	Interquartile range	0.872 (0.853 - 0.889)
LoG	6 mm	First-order	Kurtosis	1 (1 - 1)
LoG	6 mm	First-order	Maximum	0.966 (0.961 - 0.971)
LoG	6 mm	First-order	Mean absolute deviation	0.868 (0.849 - 0.886)
LoG	6 mm	First-order	Mean	0.763 (0.732 - 0.792)
LoG	6 mm	First-order	Median	0.763 (0.732 - 0.792)
LoG	6 mm	First-order	Minimum	0.835 (0.811 - 0.856)
LoG	6 mm	First-order	Range	0.869 (0.849 - 0.886)
LoG	6 mm	First-order	Robust mean absolute deviation	0.871 (0.852 - 0.888)
LoG	6 mm	First-order	Root mean squared	0.783 (0.754 - 0.81)
LoG	6 mm	First-order	Skewness	1 (1 - 1)
LoG	6 mm	First-order	Total energy	0.868 (0.849 - 0.886)
LoG	6 mm	First-order	Uniformity	0.917 (0.904 - 0.928)
LoG	6 mm	First-order	Variance	0.805 (0.778 - 0.83)
LoG	6 mm	GLCM	Autocorrelation	0.823 (0.798 - 0.846)
LoG	6 mm	GLCM	Cluster prominence	0.659 (0.619 - 0.697)
LoG	6 mm	GLCM	Cluster shade	0.756 (0.724 - 0.786)
LoG	6 mm	GLCM	Cluster tendency	0.813 (0.787 - 0.837)
LoG	6 mm	GLCM	Contrast	0.771 (0.74 - 0.799)
LoG	6 mm	GLCM	Correlation	1 (1 - 1)
LoG	6 mm	GLCM	Difference average	0.833 (0.81 - 0.855)
LoG	6 mm	GLCM	Difference entropy	0.907 (0.893 - 0.92)
LoG	6 mm	GLCM	Difference variance	0.777 (0.747 - 0.805)
LoG	6 mm	GLCM	Inverse difference	0.886 (0.869 - 0.901)
LoG	6 mm	GLCM	Inverse difference moment	0.882 (0.865 - 0.898)
LoG	6 mm	GLCM	Inverse difference moment normalized	0.995 (0.994 - 0.996)
LoG	6 mm	GLCM	Inverse difference normalized	0.997 (0.996 - 0.997)
LoG	6 mm	GLCM	Informational measure of correlation 1	0.862 (0.842 - 0.881)
LoG	6 mm	GLCM	Informational measure of correlation 2	0.732 (0.698 - 0.764)
LoG	6 mm	GLCM	Inverse variance	0.885 (0.867 - 0.9)
LoG	6 mm	GLCM	Joint average	0.883 (0.865 - 0.898)
LoG	6 mm	GLCM	Joint energy	0.967 (0.961 - 0.971)
LoG	6 mm	GLCM	Joint entropy	0.99 (0.989 - 0.992)
LoG	6 mm	GLCM	Maximal correlation coefficient	0.839 (0.816 - 0.86)
LoG	6 mm	GLCM	Maximum probability	0.947 (0.939 - 0.955)
LoG	6 mm	GLCM	Sum average	0.883 (0.865 - 0.898)
LoG	6 mm	GLCM	Sum entropy	0.965 (0.959 - 0.97)
LoG	6 mm	GLCM	Sum squares	0.807 (0.78 - 0.831)
LoG	6 mm	GLDM	Dependence entropy	0.981 (0.977 - 0.983)
LoG	6 mm	GLDM	Dependence non uniformity	0.983 (0.98 - 0.985)
LoG	6 mm	GLDM	Dependence non uniformity normalized	0.815 (0.789 - 0.838)
LoG	6 mm	GLDM	Dependence variance	0.778 (0.749 - 0.806)
LoG	6 mm	GLDM	Gray level non uniformity	0.94 (0.931 - 0.949)
LoG	6 mm	GLDM	Gray level variance	0.805 (0.778 - 0.83)
LoG	6 mm	GLDM	High gray level emphasis	0.817 (0.792 - 0.841)
LoG	6 mm	GLDM	Large dependence emphasis	0.775 (0.745 - 0.803)
LoG	6 mm	GLDM	Large dependence high gray level emphasis	0.873 (0.854 - 0.89)
LoG	6 mm	GLDM	Large dependence low gray level emphasis	0.6 (0.557 - 0.643)
LoG	6 mm	GLDM	Low gray level emphasis	0.889 (0.873 - 0.904)
LoG	6 mm	GLDM	Small dependence emphasis	0.833 (0.809 - 0.855)
LoG	6 mm	GLDM	Small dependence high gray level emphasis	0.801 (0.774 - 0.826)
LoG	6 mm	GLDM	Small dependence low gray level emphasis	0.939 (0.929 - 0.947)
LoG	6 mm	GLRLM	Gray level non uniformity	0.944 (0.935 - 0.952)
LoG	6 mm	GLRLM	Gray level non uniformity normalized	0.917 (0.905 - 0.929)
LoG	6 mm	GLRLM	Gray level variance	0.805 (0.778 - 0.83)
LoG	6 mm	GLRLM	High gray level run emphasis	0.817 (0.792 - 0.84)
LoG	6 mm	GLRLM	Long run emphasis	0.803 (0.776 - 0.828)
LoG	6 mm	GLRLM	Long run high gray level emphasis	0.82 (0.795 - 0.843)
LoG	6 mm	GLRLM	Long run low gray level emphasis	0.843 (0.821 - 0.863)
LoG	6 mm	GLRLM	Low gray level run emphasis	0.901 (0.886 - 0.914)
LoG	6 mm	GLRLM	Run entropy	0.935 (0.925 - 0.944)
LoG	6 mm	GLRLM	Run length non uniformity	0.999 (0.999 - 1)
LoG	6 mm	GLRLM	Run length non uniformity normalized	0.82 (0.796 - 0.844)
LoG	6 mm	GLRLM	Run percentage	0.816 (0.791 - 0.84)
LoG	6 mm	GLRLM	Run variance	0.801 (0.774 - 0.826)
LoG	6 mm	GLRLM	Short run emphasis	0.815 (0.79 - 0.839)
LoG	6 mm	GLRLM	Short run high gray level emphasis	0.816 (0.791 - 0.84)
LoG	6 mm	GLRLM	Short run low gray level emphasis	0.917 (0.904 - 0.929)
LoG	6 mm	GLSZM	Gray level non uniformity	0.969 (0.965 - 0.974)
LoG	6 mm	GLSZM	Gray level non uniformity normalized	0.898 (0.883 - 0.912)
LoG	6 mm	GLSZM	Gray level variance	0.801 (0.774 - 0.827)
LoG	6 mm	GLSZM	High gray level zone emphasis	0.816 (0.79 - 0.839)
LoG	6 mm	GLSZM	Large area emphasis	0.525 (0.478 - 0.572)
LoG	6 mm	GLSZM	Large area high gray level emphasis	0.864 (0.845 - 0.882)
LoG	6 mm	GLSZM	Large area low gray level emphasis	0.483 (0.434 - 0.532)
LoG	6 mm	GLSZM	Low gray level zone emphasis	0.948 (0.94 - 0.955)
LoG	6 mm	GLSZM	Size zone non uniformity	0.974 (0.97 - 0.978)
LoG	6 mm	GLSZM	Size zone non uniformity normalized	0.816 (0.791 - 0.84)
LoG	6 mm	GLSZM	Small area emphasis	0.815 (0.789 - 0.839)
LoG	6 mm	GLSZM	Small area high gray level emphasis	0.807 (0.781 - 0.832)
LoG	6 mm	GLSZM	Small area low gray level emphasis	0.867 (0.847 - 0.884)
LoG	6 mm	GLSZM	Zone entropy	0.969 (0.964 - 0.973)
LoG	6 mm	GLSZM	Zone percentage	0.834 (0.811 - 0.856)
LoG	6 mm	GLSZM	Zone variance	0.49 (0.441 - 0.538)
LoG	6 mm	NGTDM	Busyness	0.767 (0.736 - 0.796)
LoG	6 mm	NGTDM	Coarseness	0.988 (0.986 - 0.99)
LoG	6 mm	NGTDM	Complexity	0.755 (0.724 - 0.785)
LoG	6 mm	NGTDM	Contrast	0.743 (0.71 - 0.774)
LoG	6 mm	NGTDM	Strength	0.801 (0.774 - 0.826)
Wavelet	LLH	First-order	10th percentile	0.814 (0.788 - 0.838)
Wavelet	LLH	First-order	90th percentile	0.861 (0.841 - 0.88)
Wavelet	LLH	First-order	Energy	0.87 (0.851 - 0.887)
Wavelet	LLH	First-order	Entropy	0.921 (0.909 - 0.932)
Wavelet	LLH	First-order	Interquartile range	0.831 (0.807 - 0.853)
Wavelet	LLH	First-order	Kurtosis	1 (1 - 1)

Feature identifier *				
Pre-processing		Family	Feature name	ICC (95% CI)
Wavelet	LLH	First-order	Maximum	0.872 (0.853 - 0.889)
Wavelet	LLH	First-order	Mean absolute deviation	0.823 (0.798 - 0.846)
Wavelet	LLH	First-order	Mean	0.824 (0.799 - 0.847)
Wavelet	LLH	First-order	Median	0.855 (0.834 - 0.874)
Wavelet	LLH	First-order	Minimum	0.842 (0.819 - 0.862)
Wavelet	LLH	First-order	Range	0.848 (0.826 - 0.868)
Wavelet	LLH	First-order	Robust mean absolute deviation	0.827 (0.803 - 0.85)
Wavelet	LLH	First-order	Root mean squared	0.813 (0.787 - 0.837)
Wavelet	LLH	First-order	Skewness	1 (1 - 1)
Wavelet	LLH	First-order	Total energy	0.87 (0.851 - 0.887)
Wavelet	LLH	First-order	Uniformity	0.912 (0.899 - 0.924)
Wavelet	LLH	First-order	Variance	0.759 (0.727 - 0.788)
Wavelet	LLH	GLCM	Autocorrelation	0.802 (0.775 - 0.827)
Wavelet	LLH	GLCM	Cluster prominence	0.586 (0.542 - 0.63)
Wavelet	LLH	GLCM	Cluster shade	0.705 (0.669 - 0.74)
Wavelet	LLH	GLCM	Cluster tendency	0.767 (0.736 - 0.796)
Wavelet	LLH	GLCM	Contrast	0.761 (0.73 - 0.791)
Wavelet	LLH	GLCM	Correlation	1 (1 - 1)
Wavelet	LLH	GLCM	Difference average	0.816 (0.791 - 0.84)
Wavelet	LLH	GLCM	Difference entropy	0.911 (0.898 - 0.923)
Wavelet	LLH	GLCM	Difference variance	0.783 (0.754 - 0.81)
Wavelet	LLH	GLCM	Inverse difference	0.844 (0.822 - 0.865)
Wavelet	LLH	GLCM	Inverse difference moment	0.834 (0.811 - 0.856)
Wavelet	LLH	GLCM	Inverse difference moment normalized	0.999 (0.999 - 0.999)
Wavelet	LLH	GLCM	Inverse difference normalized	1 (1 - 1)
Wavelet	LLH	GLCM	Informational measure of correlation 1	0.924 (0.912 - 0.934)
Wavelet	LLH	GLCM	Informational measure of correlation 2	0.83 (0.806 - 0.852)
Wavelet	LLH	GLCM	Inverse variance	0.819 (0.794 - 0.843)
Wavelet	LLH	GLCM	Joint average	0.857 (0.837 - 0.876)
Wavelet	LLH	GLCM	Joint energy	0.996 (0.995 - 0.997)
Wavelet	LLH	GLCM	Joint entropy	0.996 (0.995 - 0.996)
Wavelet	LLH	GLCM	Maximal correlation coefficient	0.923 (0.911 - 0.933)
Wavelet	LLH	GLCM	Maximum probability	0.974 (0.97 - 0.978)
Wavelet	LLH	GLCM	Sum average	0.857 (0.837 - 0.876)
Wavelet	LLH	GLCM	Sum entropy	0.969 (0.964 - 0.973)
Wavelet	LLH	GLCM	Sum squares	0.764 (0.733 - 0.793)
Wavelet	LLH	GLDM	Dependence entropy	0.98 (0.977 - 0.983)
Wavelet	LLH	GLDM	Dependence non uniformity	0.985 (0.983 - 0.988)
Wavelet	LLH	GLDM	Dependence non uniformity normalized	0.804 (0.777 - 0.829)
Wavelet	LLH	GLDM	Dependence variance	0.766 (0.736 - 0.795)
Wavelet	LLH	GLDM	Gray level non uniformity	0.947 (0.939 - 0.954)
Wavelet	LLH	GLDM	Gray level variance	0.759 (0.727 - 0.788)
Wavelet	LLH	GLDM	High gray level emphasis	0.799 (0.771 - 0.824)
Wavelet	LLH	GLDM	Large dependence emphasis	0.767 (0.737 - 0.796)
Wavelet	LLH	GLDM	Large dependence high gray level emphasis	0.841 (0.818 - 0.862)
Wavelet	LLH	GLDM	Large dependence low gray level emphasis	0.667 (0.628 - 0.705)
Wavelet	LLH	GLDM	Low gray level emphasis	0.958 (0.951 - 0.964)
Wavelet	LLH	GLDM	Small dependence emphasis	0.806 (0.779 - 0.831)
Wavelet	LLH	GLDM	Small dependence high gray level emphasis	0.787 (0.759 - 0.814)
Wavelet	LLH	GLDM	Small dependence low gray level emphasis	0.985 (0.982 - 0.987)
Wavelet	LLH	GLRLM	Gray level non uniformity	0.949 (0.941 - 0.956)
Wavelet	LLH	GLRLM	Gray level non uniformity normalized	0.914 (0.901 - 0.926)
Wavelet	LLH	GLRLM	Gray level variance	0.759 (0.727 - 0.788)
Wavelet	LLH	GLRLM	High gray level run emphasis	0.799 (0.771 - 0.824)
Wavelet	LLH	GLRLM	Long run emphasis	0.773 (0.743 - 0.801)
Wavelet	LLH	GLRLM	Long run high gray level emphasis	0.801 (0.774 - 0.826)
Wavelet	LLH	GLRLM	Long run low gray level emphasis	0.945 (0.937 - 0.953)
Wavelet	LLH	GLRLM	Low gray level run emphasis	0.959 (0.953 - 0.965)
Wavelet	LLH	GLRLM	Run entropy	0.929 (0.918 - 0.939)
Wavelet	LLH	GLRLM	Run length non uniformity	1 (1 - 1)
Wavelet	LLH	GLRLM	Run length non uniformity normalized	0.787 (0.758 - 0.814)
Wavelet	LLH	GLRLM	Run percentage	0.783 (0.754 - 0.81)
Wavelet	LLH	GLRLM	Run variance	0.763 (0.732 - 0.793)
Wavelet	LLH	GLRLM	Short run emphasis	0.783 (0.754 - 0.81)
Wavelet	LLH	GLRLM	Short run high gray level emphasis	0.798 (0.771 - 0.824)
Wavelet	LLH	GLRLM	Short run low gray level emphasis	0.962 (0.956 - 0.968)
Wavelet	LLH	GLSZM	Gray level non uniformity	0.973 (0.969 - 0.977)
Wavelet	LLH	GLSZM	Gray level non uniformity normalized	0.921 (0.909 - 0.932)
Wavelet	LLH	GLSZM	Gray level variance	0.76 (0.729 - 0.789)
Wavelet	LLH	GLSZM	High gray level zone emphasis	0.798 (0.771 - 0.824)
Wavelet	LLH	GLSZM	Large area emphasis	0.632 (0.59 - 0.672)
Wavelet	LLH	GLSZM	Large area high gray level emphasis	0.829 (0.805 - 0.851)
Wavelet	LLH	GLSZM	Large area low gray level emphasis	0.641 (0.6 - 0.681)
Wavelet	LLH	GLSZM	Low gray level zone emphasis	0.958 (0.951 - 0.964)
Wavelet	LLH	GLSZM	Size zone non uniformity	0.982 (0.979 - 0.985)
Wavelet	LLH	GLSZM	Size zone non uniformity normalized	0.8 (0.773 - 0.825)
Wavelet	LLH	GLSZM	Small area emphasis	0.799 (0.771 - 0.824)
Wavelet	LLH	GLSZM	Small area high gray level emphasis	0.792 (0.764 - 0.819)
Wavelet	LLH	GLSZM	Small area low gray level emphasis	0.962 (0.956 - 0.967)
Wavelet	LLH	GLSZM	Zone entropy	0.969 (0.964 - 0.973)
Wavelet	LLH	GLSZM	Zone percentage	0.803 (0.776 - 0.828)
Wavelet	LLH	GLSZM	Zone variance	0.568 (0.522 - 0.613)
Wavelet	LLH	NGTDM	Busyness	0.798 (0.771 - 0.824)
Wavelet	LLH	NGTDM	Coarseness	0.969 (0.964 - 0.973)
Wavelet	LLH	NGTDM	Complexity	0.774 (0.744 - 0.802)
Wavelet	LLH	NGTDM	Contrast	0.792 (0.764 - 0.818)
Wavelet	LLH	NGTDM	Strength	0.808 (0.781 - 0.832)
Wavelet	LHL	First-order	10th percentile	0.824 (0.799 - 0.846)
Wavelet	LHL	First-order	90th percentile	0.87 (0.852 - 0.888)
Wavelet	LHL	First-order	Energy	0.876 (0.858 - 0.892)
Wavelet	LHL	First-order	Entropy	0.925 (0.914 - 0.936)
Wavelet	LHL	First-order	Interquartile range	0.842 (0.82 - 0.863)
Wavelet	LHL	First-order	Kurtosis	1 (1 - 1)
Wavelet	LHL	First-order	Maximum	0.873 (0.855 - 0.89)
Wavelet	LHL	First-order	Mean absolute deviation	0.833 (0.81 - 0.855)
Wavelet	LHL	First-order	Mean	0.816 (0.79 - 0.839)
Wavelet	LHL	First-order	Median	0.855 (0.834 - 0.874)
Wavelet	LHL	First-order	Minimum	0.855 (0.834 - 0.874)
Wavelet	LHL	First-order	Range	0.855 (0.834 - 0.874)
Wavelet	LHL	First-order	Robust mean absolute deviation	0.839 (0.816 - 0.86)
Wavelet	LHL	First-order	Root mean squared	0.82 (0.795 - 0.843)
Wavelet	LHL	First-order	Skewness	1 (1 - 1)
Wavelet	LHL	First-order	Total energy	0.876 (0.858 - 0.892)

Feature identifier *				
Pre-processing		Family	Feature name	ICC (95% CI)
Wavelet	LHL	First-order	Uniformity	0.921 (0.909 - 0.932)
Wavelet	LHL	First-order	Variance	0.774 (0.744 - 0.802)
Wavelet	LHL	GLCM	Autocorrelation	0.809 (0.783 - 0.834)
Wavelet	LHL	GLCM	Cluster prominence	0.634 (0.592 - 0.674)
Wavelet	LHL	GLCM	Cluster shade	0.755 (0.723 - 0.785)
Wavelet	LHL	GLCM	Cluster tendency	0.782 (0.753 - 0.809)
Wavelet	LHL	GLCM	Contrast	0.794 (0.766 - 0.82)
Wavelet	LHL	GLCM	Correlation	1 (1 - 1)
Wavelet	LHL	GLCM	Difference average	0.84 (0.818 - 0.861)
Wavelet	LHL	GLCM	Difference entropy	0.918 (0.905 - 0.929)
Wavelet	LHL	GLCM	Difference variance	0.803 (0.777 - 0.828)
Wavelet	LHL	GLCM	Inverse difference	0.836 (0.813 - 0.857)
Wavelet	LHL	GLCM	Inverse difference moment	0.826 (0.802 - 0.849)
Wavelet	LHL	GLCM	Inverse difference moment normalized	1 (1 - 1)
Wavelet	LHL	GLCM	Inverse difference normalized	1 (1 - 1)
Wavelet	LHL	GLCM	Informational measure of correlation 1	0.933 (0.922 - 0.942)
Wavelet	LHL	GLCM	Informational measure of correlation 2	0.837 (0.814 - 0.858)
Wavelet	LHL	GLCM	Inverse variance	0.829 (0.805 - 0.851)
Wavelet	LHL	GLCM	Joint average	0.872 (0.854 - 0.89)
Wavelet	LHL	GLCM	Joint energy	0.997 (0.997 - 0.998)
Wavelet	LHL	GLCM	Joint entropy	0.997 (0.996 - 0.997)
Wavelet	LHL	GLCM	Maximal correlation coefficient	0.927 (0.915 - 0.937)
Wavelet	LHL	GLCM	Maximum probability	0.974 (0.97 - 0.978)
Wavelet	LHL	GLCM	Sum average	0.872 (0.854 - 0.89)
Wavelet	LHL	GLCM	Sum entropy	0.973 (0.969 - 0.977)
Wavelet	LHL	GLCM	Sum squares	0.783 (0.754 - 0.81)
Wavelet	LHL	GLDM	Dependence entropy	0.981 (0.978 - 0.984)
Wavelet	LHL	GLDM	Dependence non uniformity	0.986 (0.983 - 0.988)
Wavelet	LHL	GLDM	Dependence non uniformity normalized	0.825 (0.801 - 0.848)
Wavelet	LHL	GLDM	Dependence variance	0.762 (0.731 - 0.791)
Wavelet	LHL	GLDM	Gray level non uniformity	0.948 (0.939 - 0.955)
Wavelet	LHL	GLDM	Gray level variance	0.774 (0.744 - 0.802)
Wavelet	LHL	GLDM	High gray level emphasis	0.804 (0.778 - 0.829)
Wavelet	LHL	GLDM	Large dependence emphasis	0.775 (0.745 - 0.803)
Wavelet	LHL	GLDM	Large dependence high gray level emphasis	0.845 (0.823 - 0.866)
Wavelet	LHL	GLDM	Large dependence low gray level emphasis	0.628 (0.586 - 0.669)
Wavelet	LHL	GLDM	Low gray level emphasis	0.945 (0.937 - 0.953)
Wavelet	LHL	GLDM	Small dependence emphasis	0.811 (0.784 - 0.835)
Wavelet	LHL	GLDM	Small dependence high gray level emphasis	0.794 (0.766 - 0.82)
Wavelet	LHL	GLDM	Small dependence low gray level emphasis	0.982 (0.979 - 0.984)
Wavelet	LHL	GLRLM	Gray level non uniformity	0.95 (0.943 - 0.957)
Wavelet	LHL	GLRLM	Gray level non uniformity normalized	0.923 (0.911 - 0.934)
Wavelet	LHL	GLRLM	Gray level variance	0.774 (0.744 - 0.802)
Wavelet	LHL	GLRLM	High gray level run emphasis	0.804 (0.778 - 0.829)
Wavelet	LHL	GLRLM	Long run emphasis	0.789 (0.76 - 0.815)
Wavelet	LHL	GLRLM	Long run high gray level emphasis	0.806 (0.78 - 0.831)
Wavelet	LHL	GLRLM	Long run low gray level emphasis	0.927 (0.916 - 0.937)
Wavelet	LHL	GLRLM	Low gray level run emphasis	0.949 (0.941 - 0.956)
Wavelet	LHL	GLRLM	Run entropy	0.933 (0.922 - 0.942)
Wavelet	LHL	GLRLM	Run length non uniformity	1 (1 - 1)
Wavelet	LHL	GLRLM	Run length non uniformity normalized	0.799 (0.772 - 0.825)
Wavelet	LHL	GLRLM	Run percentage	0.798 (0.771 - 0.824)
Wavelet	LHL	GLRLM	Run variance	0.79 (0.761 - 0.816)
Wavelet	LHL	GLRLM	Short run emphasis	0.795 (0.767 - 0.821)
Wavelet	LHL	GLRLM	Short run high gray level emphasis	0.804 (0.777 - 0.829)
Wavelet	LHL	GLRLM	Short run low gray level emphasis	0.954 (0.947 - 0.961)
Wavelet	LHL	GLSZM	Gray level non uniformity	0.974 (0.97 - 0.978)
Wavelet	LHL	GLSZM	Gray level non uniformity normalized	0.929 (0.918 - 0.939)
Wavelet	LHL	GLSZM	Gray level variance	0.774 (0.744 - 0.802)
Wavelet	LHL	GLSZM	High gray level zone emphasis	0.804 (0.777 - 0.829)
Wavelet	LHL	GLSZM	Large area emphasis	0.69 (0.652 - 0.726)
Wavelet	LHL	GLSZM	Large area high gray level emphasis	0.832 (0.808 - 0.853)
Wavelet	LHL	GLSZM	Large area low gray level emphasis	0.712 (0.676 - 0.746)
Wavelet	LHL	GLSZM	Low gray level zone emphasis	0.969 (0.964 - 0.973)
Wavelet	LHL	GLSZM	Size zone non uniformity	0.983 (0.981 - 0.986)
Wavelet	LHL	GLSZM	Size zone non uniformity normalized	0.805 (0.778 - 0.83)
Wavelet	LHL	GLSZM	Small area emphasis	0.794 (0.766 - 0.82)
Wavelet	LHL	GLSZM	Small area high gray level emphasis	0.799 (0.771 - 0.824)
Wavelet	LHL	GLSZM	Small area low gray level emphasis	0.961 (0.955 - 0.966)
Wavelet	LHL	GLSZM	Zone entropy	0.97 (0.965 - 0.974)
Wavelet	LHL	GLSZM	Zone percentage	0.81 (0.784 - 0.834)
Wavelet	LHL	GLSZM	Zone variance	0.636 (0.595 - 0.677)
Wavelet	LHL	NGTDM	Busyness	0.824 (0.799 - 0.846)
Wavelet	LHL	NGTDM	Coarseness	0.973 (0.969 - 0.977)
Wavelet	LHL	NGTDM	Complexity	0.782 (0.753 - 0.809)
Wavelet	LHL	NGTDM	Contrast	0.738 (0.705 - 0.77)
Wavelet	LHL	NGTDM	Strength	0.814 (0.789 - 0.838)
Wavelet	LHH	First-order	10th percentile	0.862 (0.842 - 0.88)
Wavelet	LHH	First-order	90th percentile	0.853 (0.832 - 0.872)
Wavelet	LHH	First-order	Energy	0.871 (0.853 - 0.889)
Wavelet	LHH	First-order	Entropy	0.892 (0.876 - 0.906)
Wavelet	LHH	First-order	Interquartile range	0.848 (0.827 - 0.868)
Wavelet	LHH	First-order	Kurtosis	1 (1 - 1)
Wavelet	LHH	First-order	Maximum	0.885 (0.868 - 0.901)
Wavelet	LHH	First-order	Mean absolute deviation	0.851 (0.83 - 0.871)
Wavelet	LHH	First-order	Mean	0.917 (0.904 - 0.928)
Wavelet	LHH	First-order	Median	0.952 (0.945 - 0.959)
Wavelet	LHH	First-order	Minimum	0.891 (0.874 - 0.905)
Wavelet	LHH	First-order	Range	0.885 (0.868 - 0.9)
Wavelet	LHH	First-order	Robust mean absolute deviation	0.851 (0.829 - 0.87)
Wavelet	LHH	First-order	Root mean squared	0.852 (0.831 - 0.872)
Wavelet	LHH	First-order	Skewness	1 (1 - 1)
Wavelet	LHH	First-order	Total energy	0.871 (0.853 - 0.889)
Wavelet	LHH	First-order	Uniformity	0.868 (0.849 - 0.886)
Wavelet	LHH	First-order	Variance	0.762 (0.731 - 0.791)
Wavelet	LHH	GLCM	Autocorrelation	0.833 (0.81 - 0.855)
Wavelet	LHH	GLCM	Cluster prominence	0.535 (0.488 - 0.582)
Wavelet	LHH	GLCM	Cluster shade	0.644 (0.603 - 0.684)
Wavelet	LHH	GLCM	Cluster tendency	0.756 (0.725 - 0.786)
Wavelet	LHH	GLCM	Contrast	0.77 (0.739 - 0.798)
Wavelet	LHH	GLCM	Correlation	0.998 (0.998 - 0.999)
Wavelet	LHH	GLCM	Difference average	0.858 (0.838 - 0.877)
Wavelet	LHH	GLCM	Difference entropy	0.9 (0.885 - 0.913)

Feature identifier *				
Pre-processing		Family	Feature name	ICC (95% CI)
Wavelet	LHH	GLCM	Difference variance	0.787 (0.759 - 0.814)
Wavelet	LHH	GLCM	Inverse difference	0.885 (0.868 - 0.9)
Wavelet	LHH	GLCM	Inverse difference moment	0.882 (0.864 - 0.898)
Wavelet	LHH	GLCM	Inverse difference moment normalized	0.992 (0.991 - 0.993)
Wavelet	LHH	GLCM	Inverse difference normalized	0.989 (0.987 - 0.991)
Wavelet	LHH	GLCM	Informational measure of correlation 1	0.938 (0.929 - 0.947)
Wavelet	LHH	GLCM	Informational measure of correlation 2	0.886 (0.869 - 0.902)
Wavelet	LHH	GLCM	Inverse variance	0.874 (0.856 - 0.891)
Wavelet	LHH	GLCM	Joint average	0.885 (0.868 - 0.901)
Wavelet	LHH	GLCM	Joint energy	0.844 (0.822 - 0.865)
Wavelet	LHH	GLCM	Joint entropy	0.932 (0.922 - 0.942)
Wavelet	LHH	GLCM	Maximal correlation coefficient	0.946 (0.937 - 0.953)
Wavelet	LHH	GLCM	Maximum probability	0.852 (0.831 - 0.872)
Wavelet	LHH	GLCM	Sum average	0.885 (0.868 - 0.901)
Wavelet	LHH	GLCM	Sum entropy	0.91 (0.896 - 0.922)
Wavelet	LHH	GLCM	Sum squares	0.761 (0.73 - 0.79)
Wavelet	LHH	GLDM	Dependence entropy	0.974 (0.97 - 0.977)
Wavelet	LHH	GLDM	Dependence non uniformity	0.969 (0.965 - 0.974)
Wavelet	LHH	GLDM	Dependence non uniformity normalized	0.868 (0.849 - 0.886)
Wavelet	LHH	GLDM	Dependence variance	0.827 (0.803 - 0.85)
Wavelet	LHH	GLDM	Gray level non uniformity	0.946 (0.938 - 0.954)
Wavelet	LHH	GLDM	Gray level variance	0.762 (0.73 - 0.791)
Wavelet	LHH	GLDM	High gray level emphasis	0.829 (0.805 - 0.851)
Wavelet	LHH	GLDM	Large dependence emphasis	0.814 (0.788 - 0.838)
Wavelet	LHH	GLDM	Large dependence high gray level emphasis	0.935 (0.925 - 0.944)
Wavelet	LHH	GLDM	Large dependence low gray level emphasis	0.762 (0.731 - 0.791)
Wavelet	LHH	GLDM	Low gray level emphasis	0.864 (0.844 - 0.882)
Wavelet	LHH	GLDM	Small dependence emphasis	0.872 (0.853 - 0.889)
Wavelet	LHH	GLDM	Small dependence high gray level emphasis	0.79 (0.762 - 0.816)
Wavelet	LHH	GLDM	Small dependence low gray level emphasis	0.924 (0.913 - 0.935)
Wavelet	LHH	GLRLM	Gray level non uniformity	0.959 (0.953 - 0.965)
Wavelet	LHH	GLRLM	Gray level non uniformity normalized	0.874 (0.856 - 0.891)
Wavelet	LHH	GLRLM	Gray level variance	0.763 (0.732 - 0.792)
Wavelet	LHH	GLRLM	High gray level run emphasis	0.829 (0.805 - 0.851)
Wavelet	LHH	GLRLM	Long run emphasis	0.814 (0.789 - 0.838)
Wavelet	LHH	GLRLM	Long run high gray level emphasis	0.836 (0.813 - 0.858)
Wavelet	LHH	GLRLM	Long run low gray level emphasis	0.794 (0.766 - 0.82)
Wavelet	LHH	GLRLM	Low gray level run emphasis	0.866 (0.847 - 0.884)
Wavelet	LHH	GLRLM	Run entropy	0.907 (0.892 - 0.919)
Wavelet	LHH	GLRLM	Run length non uniformity	0.996 (0.996 - 0.997)
Wavelet	LHH	GLRLM	Run length non uniformity normalized	0.862 (0.842 - 0.88)
Wavelet	LHH	GLRLM	Run percentage	0.855 (0.834 - 0.874)
Wavelet	LHH	GLRLM	Run variance	0.814 (0.789 - 0.838)
Wavelet	LHH	GLRLM	Short run emphasis	0.851 (0.83 - 0.871)
Wavelet	LHH	GLRLM	Short run high gray level emphasis	0.827 (0.803 - 0.849)
Wavelet	LHH	GLRLM	Short run low gray level emphasis	0.884 (0.867 - 0.9)
Wavelet	LHH	GLSZM	Gray level non uniformity	0.986 (0.984 - 0.988)
Wavelet	LHH	GLSZM	Gray level non uniformity normalized	0.89 (0.873 - 0.905)
Wavelet	LHH	GLSZM	Gray level variance	0.776 (0.746 - 0.804)
Wavelet	LHH	GLSZM	High gray level zone emphasis	0.83 (0.806 - 0.852)
Wavelet	LHH	GLSZM	Large area emphasis	0.62 (0.577 - 0.661)
Wavelet	LHH	GLSZM	Large area high gray level emphasis	0.782 (0.753 - 0.81)
Wavelet	LHH	GLSZM	Large area low gray level emphasis	0.55 (0.504 - 0.596)
Wavelet	LHH	GLSZM	Low gray level zone emphasis	0.888 (0.871 - 0.903)
Wavelet	LHH	GLSZM	Size zone non uniformity	0.944 (0.935 - 0.952)
Wavelet	LHH	GLSZM	Size zone non uniformity normalized	0.847 (0.825 - 0.867)
Wavelet	LHH	GLSZM	Small area emphasis	0.839 (0.817 - 0.86)
Wavelet	LHH	GLSZM	Small area high gray level emphasis	0.813 (0.787 - 0.837)
Wavelet	LHH	GLSZM	Small area low gray level emphasis	0.801 (0.774 - 0.826)
Wavelet	LHH	GLSZM	Zone entropy	0.949 (0.941 - 0.956)
Wavelet	LHH	GLSZM	Zone percentage	0.876 (0.858 - 0.892)
Wavelet	LHH	GLSZM	Zone variance	0.614 (0.571 - 0.656)
Wavelet	LHH	NGTDM	Busyness	0.812 (0.786 - 0.836)
Wavelet	LHH	NGTDM	Coarseness	0.988 (0.986 - 0.989)
Wavelet	LHH	NGTDM	Complexity	0.773 (0.743 - 0.802)
Wavelet	LHH	NGTDM	Contrast	0.78 (0.751 - 0.807)
Wavelet	LHH	NGTDM	Strength	0.831 (0.808 - 0.853)
Wavelet	HLL	First-order	10th percentile	0.817 (0.792 - 0.841)
Wavelet	HLL	First-order	90th percentile	0.871 (0.852 - 0.888)
Wavelet	HLL	First-order	Energy	0.873 (0.854 - 0.89)
Wavelet	HLL	First-order	Entropy	0.923 (0.911 - 0.934)
Wavelet	HLL	First-order	Interquartile range	0.846 (0.824 - 0.866)
Wavelet	HLL	First-order	Kurtosis	1 (1 - 1)
Wavelet	HLL	First-order	Maximum	0.88 (0.863 - 0.897)
Wavelet	HLL	First-order	Mean absolute deviation	0.832 (0.808 - 0.854)
Wavelet	HLL	First-order	Mean	0.809 (0.783 - 0.833)
Wavelet	HLL	First-order	Median	0.858 (0.837 - 0.877)
Wavelet	HLL	First-order	Minimum	0.851 (0.83 - 0.871)
Wavelet	HLL	First-order	Range	0.854 (0.833 - 0.873)
Wavelet	HLL	First-order	Robust mean absolute deviation	0.839 (0.817 - 0.86)
Wavelet	HLL	First-order	Root mean squared	0.818 (0.793 - 0.841)
Wavelet	HLL	First-order	Skewness	1 (1 - 1)
Wavelet	HLL	First-order	Total energy	0.873 (0.854 - 0.89)
Wavelet	HLL	First-order	Uniformity	0.916 (0.903 - 0.928)
Wavelet	HLL	First-order	Variance	0.795 (0.767 - 0.821)
Wavelet	HLL	GLCM	Autocorrelation	0.822 (0.797 - 0.845)
Wavelet	HLL	GLCM	Cluster prominence	0.734 (0.7 - 0.766)
Wavelet	HLL	GLCM	Cluster shade	0.814 (0.788 - 0.837)
Wavelet	HLL	GLCM	Cluster tendency	0.807 (0.78 - 0.831)
Wavelet	HLL	GLCM	Contrast	0.794 (0.766 - 0.82)
Wavelet	HLL	GLCM	Correlation	1 (1 - 1)
Wavelet	HLL	GLCM	Difference average	0.833 (0.81 - 0.855)
Wavelet	HLL	GLCM	Difference entropy	0.915 (0.902 - 0.926)
Wavelet	HLL	GLCM	Difference variance	0.814 (0.788 - 0.838)
Wavelet	HLL	GLCM	Inverse difference	0.842 (0.82 - 0.863)
Wavelet	HLL	GLCM	Inverse difference moment	0.831 (0.807 - 0.853)
Wavelet	HLL	GLCM	Inverse difference moment normalized	1 (1 - 1)
Wavelet	HLL	GLCM	Inverse difference normalized	1 (1 - 1)
Wavelet	HLL	GLCM	Informational measure of correlation 1	0.931 (0.92 - 0.941)
Wavelet	HLL	GLCM	Informational measure of correlation 2	0.828 (0.804 - 0.85)
Wavelet	HLL	GLCM	Inverse variance	0.832 (0.809 - 0.854)
Wavelet	HLL	GLCM	Joint average	0.868 (0.849 - 0.886)
Wavelet	HLL	GLCM	Joint energy	0.996 (0.995 - 0.997)

Feature identifier *				
Pre-processing		Family	Feature name	ICC (95% CI)
Wavelet	HLL	GLCM	Joint entropy	0.996 (0.995 - 0.996)
Wavelet	HLL	GLCM	Maximal correlation coefficient	0.929 (0.918 - 0.939)
Wavelet	HLL	GLCM	Maximum probability	0.974 (0.97 - 0.978)
Wavelet	HLL	GLCM	Sum average	0.868 (0.849 - 0.886)
Wavelet	HLL	GLCM	Sum entropy	0.972 (0.967 - 0.976)
Wavelet	HLL	GLCM	Sum squares	0.802 (0.775 - 0.827)
Wavelet	HLL	GLDM	Dependence entropy	0.982 (0.979 - 0.984)
Wavelet	HLL	GLDM	Dependence non uniformity	0.983 (0.981 - 0.986)
Wavelet	HLL	GLDM	Dependence non uniformity normalized	0.806 (0.78 - 0.831)
Wavelet	HLL	GLDM	Dependence variance	0.766 (0.735 - 0.794)
Wavelet	HLL	GLDM	Gray level non uniformity	0.946 (0.938 - 0.954)
Wavelet	HLL	GLDM	Gray level variance	0.795 (0.767 - 0.821)
Wavelet	HLL	GLDM	High gray level emphasis	0.819 (0.793 - 0.842)
Wavelet	HLL	GLDM	Large dependence emphasis	0.766 (0.735 - 0.795)
Wavelet	HLL	GLDM	Large dependence high gray level emphasis	0.859 (0.839 - 0.878)
Wavelet	HLL	GLDM	Large dependence low gray level emphasis	0.781 (0.752 - 0.809)
Wavelet	HLL	GLDM	Low gray level emphasis	0.974 (0.97 - 0.977)
Wavelet	HLL	GLDM	Small dependence emphasis	0.802 (0.775 - 0.827)
Wavelet	HLL	GLDM	Small dependence high gray level emphasis	0.807 (0.78 - 0.831)
Wavelet	HLL	GLDM	Small dependence low gray level emphasis	0.981 (0.978 - 0.984)
Wavelet	HLL	GLRLM	Gray level non uniformity	0.949 (0.941 - 0.957)
Wavelet	HLL	GLRLM	Gray level non uniformity normalized	0.917 (0.904 - 0.928)
Wavelet	HLL	GLRLM	Gray level variance	0.795 (0.767 - 0.821)
Wavelet	HLL	GLRLM	High gray level run emphasis	0.819 (0.793 - 0.842)
Wavelet	HLL	GLRLM	Long run emphasis	0.783 (0.754 - 0.81)
Wavelet	HLL	GLRLM	Long run high gray level emphasis	0.821 (0.796 - 0.844)
Wavelet	HLL	GLRLM	Long run low gray level emphasis	0.965 (0.959 - 0.97)
Wavelet	HLL	GLRLM	Low gray level run emphasis	0.975 (0.971 - 0.979)
Wavelet	HLL	GLRLM	Run entropy	0.931 (0.92 - 0.94)
Wavelet	HLL	GLRLM	Run length non uniformity	1 (1 - 1)
Wavelet	HLL	GLRLM	Run length non uniformity normalized	0.788 (0.759 - 0.814)
Wavelet	HLL	GLRLM	Run percentage	0.787 (0.758 - 0.814)
Wavelet	HLL	GLRLM	Run variance	0.788 (0.759 - 0.814)
Wavelet	HLL	GLRLM	Short run emphasis	0.783 (0.754 - 0.81)
Wavelet	HLL	GLRLM	Short run high gray level emphasis	0.818 (0.793 - 0.841)
Wavelet	HLL	GLRLM	Short run low gray level emphasis	0.978 (0.974 - 0.981)
Wavelet	HLL	GLSZM	Gray level non uniformity	0.977 (0.973 - 0.98)
Wavelet	HLL	GLSZM	Gray level non uniformity normalized	0.924 (0.912 - 0.935)
Wavelet	HLL	GLSZM	Gray level variance	0.796 (0.768 - 0.822)
Wavelet	HLL	GLSZM	High gray level zone emphasis	0.818 (0.793 - 0.841)
Wavelet	HLL	GLSZM	Large area emphasis	0.66 (0.62 - 0.698)
Wavelet	HLL	GLSZM	Large area high gray level emphasis	0.848 (0.827 - 0.868)
Wavelet	HLL	GLSZM	Large area low gray level emphasis	0.704 (0.668 - 0.739)
Wavelet	HLL	GLSZM	Low gray level zone emphasis	0.97 (0.965 - 0.974)
Wavelet	HLL	GLSZM	Size zone non uniformity	0.98 (0.977 - 0.983)
Wavelet	HLL	GLSZM	Size zone non uniformity normalized	0.794 (0.767 - 0.82)
Wavelet	HLL	GLSZM	Small area emphasis	0.785 (0.756 - 0.812)
Wavelet	HLL	GLSZM	Small area high gray level emphasis	0.812 (0.786 - 0.836)
Wavelet	HLL	GLSZM	Small area low gray level emphasis	0.952 (0.944 - 0.958)
Wavelet	HLL	GLSZM	Zone entropy	0.971 (0.966 - 0.975)
Wavelet	HLL	GLSZM	Zone percentage	0.799 (0.772 - 0.824)
Wavelet	HLL	GLSZM	Zone variance	0.638 (0.596 - 0.678)
Wavelet	HLL	NGTDM	Busyness	0.818 (0.793 - 0.841)
Wavelet	HLL	NGTDM	Coarseness	0.971 (0.966 - 0.975)
Wavelet	HLL	NGTDM	Complexity	0.805 (0.779 - 0.83)
Wavelet	HLL	NGTDM	Contrast	0.895 (0.88 - 0.91)
Wavelet	HLL	NGTDM	Strength	0.824 (0.8 - 0.847)
Wavelet	HLH	First-order	10th percentile	0.847 (0.826 - 0.867)
Wavelet	HLH	First-order	90th percentile	0.835 (0.812 - 0.856)
Wavelet	HLH	First-order	Energy	0.879 (0.861 - 0.895)
Wavelet	HLH	First-order	Entropy	0.873 (0.854 - 0.89)
Wavelet	HLH	First-order	Interquartile range	0.841 (0.819 - 0.862)
Wavelet	HLH	First-order	Kurtosis	1 (1 - 1)
Wavelet	HLH	First-order	Maximum	0.889 (0.873 - 0.904)
Wavelet	HLH	First-order	Mean absolute deviation	0.839 (0.816 - 0.86)
Wavelet	HLH	First-order	Mean	0.897 (0.882 - 0.911)
Wavelet	HLH	First-order	Median	0.949 (0.941 - 0.956)
Wavelet	HLH	First-order	Minimum	0.885 (0.868 - 0.9)
Wavelet	HLH	First-order	Range	0.884 (0.867 - 0.9)
Wavelet	HLH	First-order	Robust mean absolute deviation	0.839 (0.817 - 0.86)
Wavelet	HLH	First-order	Root mean squared	0.841 (0.818 - 0.862)
Wavelet	HLH	First-order	Skewness	1 (1 - 1)
Wavelet	HLH	First-order	Total energy	0.879 (0.861 - 0.895)
Wavelet	HLH	First-order	Uniformity	0.852 (0.831 - 0.872)
Wavelet	HLH	First-order	Variance	0.775 (0.745 - 0.803)
Wavelet	HLH	GLCM	Autocorrelation	0.83 (0.806 - 0.852)
Wavelet	HLH	GLCM	Cluster prominence	0.574 (0.529 - 0.618)
Wavelet	HLH	GLCM	Cluster shade	0.685 (0.647 - 0.721)
Wavelet	HLH	GLCM	Cluster tendency	0.765 (0.735 - 0.794)
Wavelet	HLH	GLCM	Contrast	0.789 (0.761 - 0.816)
Wavelet	HLH	GLCM	Correlation	0.998 (0.998 - 0.998)
Wavelet	HLH	GLCM	Difference average	0.847 (0.826 - 0.867)
Wavelet	HLH	GLCM	Difference entropy	0.885 (0.868 - 0.901)
Wavelet	HLH	GLCM	Difference variance	0.805 (0.779 - 0.83)
Wavelet	HLH	GLCM	Inverse difference	0.869 (0.849 - 0.886)
Wavelet	HLH	GLCM	Inverse difference moment	0.868 (0.849 - 0.886)
Wavelet	HLH	GLCM	Inverse difference moment normalized	0.988 (0.986 - 0.989)
Wavelet	HLH	GLCM	Inverse difference normalized	0.99 (0.989 - 0.992)
Wavelet	HLH	GLCM	Informational measure of correlation 1	0.925 (0.914 - 0.936)
Wavelet	HLH	GLCM	Informational measure of correlation 2	0.884 (0.867 - 0.9)
Wavelet	HLH	GLCM	Inverse variance	0.863 (0.843 - 0.881)
Wavelet	HLH	GLCM	Joint average	0.878 (0.86 - 0.895)
Wavelet	HLH	GLCM	Joint energy	0.852 (0.83 - 0.871)
Wavelet	HLH	GLCM	Joint entropy	0.922 (0.91 - 0.933)
Wavelet	HLH	GLCM	Maximal correlation coefficient	0.935 (0.925 - 0.944)
Wavelet	HLH	GLCM	Maximum probability	0.858 (0.837 - 0.877)
Wavelet	HLH	GLCM	Sum average	0.878 (0.86 - 0.895)
Wavelet	HLH	GLCM	Sum entropy	0.895 (0.879 - 0.909)
Wavelet	HLH	GLCM	Sum squares	0.774 (0.744 - 0.802)
Wavelet	HLH	GLDM	Dependence entropy	0.974 (0.969 - 0.977)
Wavelet	HLH	GLDM	Dependence non uniformity	0.969 (0.964 - 0.973)
Wavelet	HLH	GLDM	Dependence non uniformity normalized	0.851 (0.83 - 0.871)
Wavelet	HLH	GLDM	Dependence variance	0.815 (0.789 - 0.839)

Feature identifier *				
Pre-processing		Family	Feature name	ICC (95% CI)
Wavelet	HLH	GLDM	Gray level non uniformity	0.95 (0.942 - 0.957)
Wavelet	HLH	GLDM	Gray level variance	0.774 (0.744 - 0.802)
Wavelet	HLH	GLDM	High gray level emphasis	0.828 (0.804 - 0.85)
Wavelet	HLH	GLDM	Large dependence emphasis	0.811 (0.785 - 0.835)
Wavelet	HLH	GLDM	Large dependence high gray level emphasis	0.928 (0.917 - 0.938)
Wavelet	HLH	GLDM	Large dependence low gray level emphasis	0.701 (0.664 - 0.736)
Wavelet	HLH	GLDM	Low gray level emphasis	0.855 (0.835 - 0.875)
Wavelet	HLH	GLDM	Small dependence emphasis	0.849 (0.827 - 0.869)
Wavelet	HLH	GLDM	Small dependence high gray level emphasis	0.793 (0.765 - 0.819)
Wavelet	HLH	GLDM	Small dependence low gray level emphasis	0.953 (0.946 - 0.96)
Wavelet	HLH	GLRLM	Gray level non uniformity	0.962 (0.956 - 0.968)
Wavelet	HLH	GLRLM	Gray level non uniformity normalized	0.857 (0.836 - 0.876)
Wavelet	HLH	GLRLM	Gray level variance	0.775 (0.746 - 0.803)
Wavelet	HLH	GLRLM	High gray level run emphasis	0.828 (0.804 - 0.85)
Wavelet	HLH	GLRLM	Long run emphasis	0.82 (0.795 - 0.843)
Wavelet	HLH	GLRLM	Long run high gray level emphasis	0.835 (0.812 - 0.856)
Wavelet	HLH	GLRLM	Long run low gray level emphasis	0.787 (0.759 - 0.814)
Wavelet	HLH	GLRLM	Low gray level run emphasis	0.858 (0.838 - 0.877)
Wavelet	HLH	GLRLM	Run entropy	0.891 (0.875 - 0.906)
Wavelet	HLH	GLRLM	Run length non uniformity	0.995 (0.995 - 0.996)
Wavelet	HLH	GLRLM	Run length non uniformity normalized	0.852 (0.831 - 0.871)
Wavelet	HLH	GLRLM	Run percentage	0.847 (0.825 - 0.867)
Wavelet	HLH	GLRLM	Run variance	0.82 (0.795 - 0.843)
Wavelet	HLH	GLRLM	Short run emphasis	0.843 (0.821 - 0.864)
Wavelet	HLH	GLRLM	Short run high gray level emphasis	0.826 (0.802 - 0.849)
Wavelet	HLH	GLRLM	Short run low gray level emphasis	0.874 (0.856 - 0.891)
Wavelet	HLH	GLSZM	Gray level non uniformity	0.987 (0.985 - 0.989)
Wavelet	HLH	GLSZM	Gray level non uniformity normalized	0.876 (0.858 - 0.893)
Wavelet	HLH	GLSZM	Gray level variance	0.791 (0.763 - 0.817)
Wavelet	HLH	GLSZM	High gray level zone emphasis	0.828 (0.804 - 0.851)
Wavelet	HLH	GLSZM	Large area emphasis	0.664 (0.624 - 0.702)
Wavelet	HLH	GLSZM	Large area high gray level emphasis	0.896 (0.881 - 0.91)
Wavelet	HLH	GLSZM	Large area low gray level emphasis	0.494 (0.446 - 0.543)
Wavelet	HLH	GLSZM	Low gray level zone emphasis	0.866 (0.846 - 0.884)
Wavelet	HLH	GLSZM	Size zone non uniformity	0.939 (0.93 - 0.948)
Wavelet	HLH	GLSZM	Size zone non uniformity normalized	0.821 (0.796 - 0.844)
Wavelet	HLH	GLSZM	Small area emphasis	0.822 (0.797 - 0.845)
Wavelet	HLH	GLSZM	Small area high gray level emphasis	0.813 (0.787 - 0.837)
Wavelet	HLH	GLSZM	Small area low gray level emphasis	0.842 (0.819 - 0.862)
Wavelet	HLH	GLSZM	Zone entropy	0.949 (0.941 - 0.956)
Wavelet	HLH	GLSZM	Zone percentage	0.853 (0.832 - 0.872)
Wavelet	HLH	GLSZM	Zone variance	0.669 (0.63 - 0.707)
Wavelet	HLH	NGTDM	Busyness	0.745 (0.712 - 0.776)
Wavelet	HLH	NGTDM	Coarseness	0.995 (0.994 - 0.996)
Wavelet	HLH	NGTDM	Complexity	0.801 (0.774 - 0.827)
Wavelet	HLH	NGTDM	Contrast	0.795 (0.767 - 0.821)
Wavelet	HLH	NGTDM	Strength	0.811 (0.785 - 0.835)
Wavelet	HHL	First-order	10th percentile	0.881 (0.864 - 0.897)
Wavelet	HHL	First-order	90th percentile	0.861 (0.841 - 0.879)
Wavelet	HHL	First-order	Energy	0.905 (0.89 - 0.918)
Wavelet	HHL	First-order	Entropy	0.884 (0.867 - 0.9)
Wavelet	HHL	First-order	Interquartile range	0.87 (0.851 - 0.887)
Wavelet	HHL	First-order	Kurtosis	1 (1 - 1)
Wavelet	HHL	First-order	Maximum	0.894 (0.878 - 0.908)
Wavelet	HHL	First-order	Mean absolute deviation	0.864 (0.844 - 0.882)
Wavelet	HHL	First-order	Mean	0.917 (0.904 - 0.928)
Wavelet	HHL	First-order	Median	0.953 (0.946 - 0.96)
Wavelet	HHL	First-order	Minimum	0.897 (0.882 - 0.911)
Wavelet	HHL	First-order	Range	0.891 (0.875 - 0.906)
Wavelet	HHL	First-order	Robust mean absolute deviation	0.868 (0.849 - 0.886)
Wavelet	HHL	First-order	Root mean squared	0.862 (0.843 - 0.881)
Wavelet	HHL	First-order	Skewness	1 (1 - 1)
Wavelet	HHL	First-order	Total energy	0.905 (0.89 - 0.918)
Wavelet	HHL	First-order	Uniformity	0.857 (0.837 - 0.876)
Wavelet	HHL	First-order	Variance	0.834 (0.81 - 0.855)
Wavelet	HHL	GLCM	Autocorrelation	0.867 (0.848 - 0.885)
Wavelet	HHL	GLCM	Cluster prominence	0.789 (0.761 - 0.816)
Wavelet	HHL	GLCM	Cluster shade	0.78 (0.751 - 0.807)
Wavelet	HHL	GLCM	Cluster tendency	0.825 (0.801 - 0.848)
Wavelet	HHL	GLCM	Contrast	0.838 (0.816 - 0.859)
Wavelet	HHL	GLCM	Correlation	0.998 (0.998 - 0.998)
Wavelet	HHL	GLCM	Difference average	0.87 (0.851 - 0.887)
Wavelet	HHL	GLCM	Difference entropy	0.894 (0.878 - 0.908)
Wavelet	HHL	GLCM	Difference variance	0.844 (0.822 - 0.865)
Wavelet	HHL	GLCM	Inverse difference	0.88 (0.862 - 0.896)
Wavelet	HHL	GLCM	Inverse difference moment	0.876 (0.858 - 0.893)
Wavelet	HHL	GLCM	Inverse difference moment normalized	0.993 (0.992 - 0.994)
Wavelet	HHL	GLCM	Inverse difference normalized	0.993 (0.992 - 0.994)
Wavelet	HHL	GLCM	Informational measure of correlation 1	0.936 (0.926 - 0.945)
Wavelet	HHL	GLCM	Informational measure of correlation 2	0.885 (0.868 - 0.901)
Wavelet	HHL	GLCM	Inverse variance	0.875 (0.857 - 0.892)
Wavelet	HHL	GLCM	Joint average	0.891 (0.875 - 0.906)
Wavelet	HHL	GLCM	Joint energy	0.852 (0.83 - 0.871)
Wavelet	HHL	GLCM	Joint entropy	0.925 (0.913 - 0.935)
Wavelet	HHL	GLCM	Maximal correlation coefficient	0.944 (0.935 - 0.952)
Wavelet	HHL	GLCM	Maximum probability	0.858 (0.837 - 0.877)
Wavelet	HHL	GLCM	Sum average	0.891 (0.875 - 0.906)
Wavelet	HHL	GLCM	Sum entropy	0.901 (0.887 - 0.915)
Wavelet	HHL	GLCM	Sum squares	0.83 (0.806 - 0.852)
Wavelet	HHL	GLDM	Dependence entropy	0.972 (0.968 - 0.976)
Wavelet	HHL	GLDM	Dependence non uniformity	0.968 (0.963 - 0.973)
Wavelet	HHL	GLDM	Dependence non uniformity normalized	0.878 (0.86 - 0.894)
Wavelet	HHL	GLDM	Dependence variance	0.847 (0.826 - 0.867)
Wavelet	HHL	GLDM	Gray level non uniformity	0.955 (0.948 - 0.961)
Wavelet	HHL	GLDM	Gray level variance	0.834 (0.81 - 0.855)
Wavelet	HHL	GLDM	High gray level emphasis	0.867 (0.847 - 0.885)
Wavelet	HHL	GLDM	Large dependence emphasis	0.83 (0.806 - 0.852)
Wavelet	HHL	GLDM	Large dependence high gray level emphasis	0.947 (0.939 - 0.955)
Wavelet	HHL	GLDM	Large dependence low gray level emphasis	0.728 (0.694 - 0.761)
Wavelet	HHL	GLDM	Low gray level emphasis	0.896 (0.881 - 0.911)
Wavelet	HHL	GLDM	Small dependence emphasis	0.871 (0.852 - 0.888)
Wavelet	HHL	GLDM	Small dependence high gray level emphasis	0.844 (0.822 - 0.865)
Wavelet	HHL	GLDM	Small dependence low gray level emphasis	0.937 (0.927 - 0.946)

Feature identifier *				
Pre-processing		Family	Feature name	ICC (95% CI)
Wavelet	HHL	GLRLM	Gray level non uniformity	0.967 (0.962 - 0.972)
Wavelet	HHL	GLRLM	Gray level non uniformity normalized	0.861 (0.841 - 0.88)
Wavelet	HHL	GLRLM	Gray level variance	0.834 (0.811 - 0.856)
Wavelet	HHL	GLRLM	High gray level run emphasis	0.867 (0.847 - 0.885)
Wavelet	HHL	GLRLM	Long run emphasis	0.833 (0.809 - 0.854)
Wavelet	HHL	GLRLM	Long run high gray level emphasis	0.872 (0.854 - 0.889)
Wavelet	HHL	GLRLM	Long run low gray level emphasis	0.836 (0.813 - 0.857)
Wavelet	HHL	GLRLM	Low gray level run emphasis	0.895 (0.879 - 0.909)
Wavelet	HHL	GLRLM	Run entropy	0.9 (0.885 - 0.914)
Wavelet	HHL	GLRLM	Run length non uniformity	0.995 (0.994 - 0.995)
Wavelet	HHL	GLRLM	Run length non uniformity normalized	0.863 (0.843 - 0.881)
Wavelet	HHL	GLRLM	Run percentage	0.86 (0.84 - 0.878)
Wavelet	HHL	GLRLM	Run variance	0.839 (0.816 - 0.86)
Wavelet	HHL	GLRLM	Short run emphasis	0.849 (0.828 - 0.869)
Wavelet	HHL	GLRLM	Short run high gray level emphasis	0.866 (0.846 - 0.884)
Wavelet	HHL	GLRLM	Short run low gray level emphasis	0.906 (0.891 - 0.918)
Wavelet	HHL	GLSZM	Gray level non uniformity	0.985 (0.982 - 0.987)
Wavelet	HHL	GLSZM	Gray level non uniformity normalized	0.857 (0.836 - 0.876)
Wavelet	HHL	GLSZM	Gray level variance	0.841 (0.818 - 0.862)
Wavelet	HHL	GLSZM	High gray level zone emphasis	0.867 (0.848 - 0.885)
Wavelet	HHL	GLSZM	Large area emphasis	0.774 (0.744 - 0.802)
Wavelet	HHL	GLSZM	Large area high gray level emphasis	0.938 (0.928 - 0.947)
Wavelet	HHL	GLSZM	Large area low gray level emphasis	0.588 (0.544 - 0.632)
Wavelet	HHL	GLSZM	Low gray level zone emphasis	0.864 (0.844 - 0.882)
Wavelet	HHL	GLSZM	Size zone non uniformity	0.94 (0.93 - 0.948)
Wavelet	HHL	GLSZM	Size zone non uniformity normalized	0.843 (0.821 - 0.864)
Wavelet	HHL	GLSZM	Small area emphasis	0.85 (0.829 - 0.87)
Wavelet	HHL	GLSZM	Small area high gray level emphasis	0.857 (0.836 - 0.876)
Wavelet	HHL	GLSZM	Small area low gray level emphasis	0.797 (0.77 - 0.823)
Wavelet	HHL	GLSZM	Zone entropy	0.937 (0.927 - 0.946)
Wavelet	HHL	GLSZM	Zone percentage	0.874 (0.855 - 0.891)
Wavelet	HHL	GLSZM	Zone variance	0.777 (0.748 - 0.805)
Wavelet	HHL	NGTDM	Busyness	0.734 (0.7 - 0.766)
Wavelet	HHL	NGTDM	Coarseness	0.992 (0.991 - 0.993)
Wavelet	HHL	NGTDM	Complexity	0.88 (0.862 - 0.896)
Wavelet	HHL	NGTDM	Contrast	0.905 (0.891 - 0.918)
Wavelet	HHL	NGTDM	Strength	0.852 (0.83 - 0.871)
Wavelet	HHH	First-order	10th percentile	0.898 (0.883 - 0.912)
Wavelet	HHH	First-order	90th percentile	0.902 (0.887 - 0.915)
Wavelet	HHH	First-order	Energy	0.903 (0.888 - 0.916)
Wavelet	HHH	First-order	Entropy	0.909 (0.896 - 0.922)
Wavelet	HHH	First-order	Interquartile range	0.896 (0.881 - 0.911)
Wavelet	HHH	First-order	Kurtosis	1 (1 - 1)
Wavelet	HHH	First-order	Maximum	0.926 (0.914 - 0.936)
Wavelet	HHH	First-order	Mean absolute deviation	0.899 (0.884 - 0.913)
Wavelet	HHH	First-order	Mean	0.948 (0.94 - 0.955)
Wavelet	HHH	First-order	Median	0.961 (0.955 - 0.967)
Wavelet	HHH	First-order	Minimum	0.929 (0.918 - 0.939)
Wavelet	HHH	First-order	Range	0.926 (0.915 - 0.937)
Wavelet	HHH	First-order	Robust mean absolute deviation	0.897 (0.881 - 0.911)
Wavelet	HHH	First-order	Root mean squared	0.902 (0.887 - 0.915)
Wavelet	HHH	First-order	Skewness	1 (1 - 1)
Wavelet	HHH	First-order	Total energy	0.903 (0.888 - 0.916)
Wavelet	HHH	First-order	Uniformity	0.907 (0.893 - 0.92)
Wavelet	HHH	First-order	Variance	0.843 (0.821 - 0.864)
Wavelet	HHH	GLCM	Autocorrelation	0.89 (0.873 - 0.905)
Wavelet	HHH	GLCM	Cluster prominence	0.635 (0.593 - 0.675)
Wavelet	HHH	GLCM	Cluster shade	0.755 (0.723 - 0.785)
Wavelet	HHH	GLCM	Cluster tendency	0.837 (0.814 - 0.858)
Wavelet	HHH	GLCM	Contrast	0.85 (0.828 - 0.87)
Wavelet	HHH	GLCM	Correlation	0.991 (0.989 - 0.992)
Wavelet	HHH	GLCM	Difference average	0.899 (0.884 - 0.913)
Wavelet	HHH	GLCM	Difference entropy	0.915 (0.902 - 0.927)
Wavelet	HHH	GLCM	Difference variance	0.862 (0.842 - 0.88)
Wavelet	HHH	GLCM	Inverse difference	0.913 (0.899 - 0.925)
Wavelet	HHH	GLCM	Inverse difference moment	0.91 (0.897 - 0.923)
Wavelet	HHH	GLCM	Inverse difference moment normalized	0.868 (0.849 - 0.886)
Wavelet	HHH	GLCM	Inverse difference normalized	0.928 (0.917 - 0.938)
Wavelet	HHH	GLCM	Informational measure of correlation 1	0.928 (0.917 - 0.938)
Wavelet	HHH	GLCM	Informational measure of correlation 2	0.901 (0.886 - 0.915)
Wavelet	HHH	GLCM	Inverse variance	0.856 (0.835 - 0.875)
Wavelet	HHH	GLCM	Joint average	0.929 (0.918 - 0.938)
Wavelet	HHH	GLCM	Joint energy	0.915 (0.902 - 0.927)
Wavelet	HHH	GLCM	Joint entropy	0.915 (0.903 - 0.927)
Wavelet	HHH	GLCM	Maximal correlation coefficient	0.925 (0.913 - 0.935)
Wavelet	HHH	GLCM	Maximum probability	0.925 (0.914 - 0.936)
Wavelet	HHH	GLCM	Sum average	0.929 (0.918 - 0.938)
Wavelet	HHH	GLCM	Sum entropy	0.909 (0.896 - 0.922)
Wavelet	HHH	GLCM	Sum squares	0.843 (0.821 - 0.864)
Wavelet	HHH	GLDM	Dependence entropy	0.961 (0.954 - 0.966)
Wavelet	HHH	GLDM	Dependence non uniformity	0.975 (0.971 - 0.979)
Wavelet	HHH	GLDM	Dependence non uniformity normalized	0.901 (0.886 - 0.914)
Wavelet	HHH	GLDM	Dependence variance	0.926 (0.915 - 0.936)
Wavelet	HHH	GLDM	Gray level non uniformity	0.981 (0.977 - 0.983)
Wavelet	HHH	GLDM	Gray level variance	0.843 (0.821 - 0.864)
Wavelet	HHH	GLDM	High gray level emphasis	0.889 (0.872 - 0.904)
Wavelet	HHH	GLDM	Large dependence emphasis	0.929 (0.918 - 0.939)
Wavelet	HHH	GLDM	Large dependence high gray level emphasis	0.965 (0.959 - 0.97)
Wavelet	HHH	GLDM	Large dependence low gray level emphasis	0.832 (0.809 - 0.854)
Wavelet	HHH	GLDM	Low gray level emphasis	0.843 (0.821 - 0.864)
Wavelet	HHH	GLDM	Small dependence emphasis	0.894 (0.878 - 0.909)
Wavelet	HHH	GLDM	Small dependence high gray level emphasis	0.818 (0.793 - 0.841)
Wavelet	HHH	GLDM	Small dependence low gray level emphasis	0.926 (0.915 - 0.936)
Wavelet	HHH	GLRLM	Gray level non uniformity	0.988 (0.986 - 0.99)
Wavelet	HHH	GLRLM	Gray level non uniformity normalized	0.908 (0.895 - 0.921)
Wavelet	HHH	GLRLM	Gray level variance	0.847 (0.825 - 0.867)
Wavelet	HHH	GLRLM	High gray level run emphasis	0.889 (0.872 - 0.904)
Wavelet	HHH	GLRLM	Long run emphasis	0.929 (0.918 - 0.939)
Wavelet	HHH	GLRLM	Long run high gray level emphasis	0.909 (0.895 - 0.921)
Wavelet	HHH	GLRLM	Long run low gray level emphasis	0.831 (0.808 - 0.853)
Wavelet	HHH	GLRLM	Low gray level run emphasis	0.846 (0.824 - 0.866)
Wavelet	HHH	GLRLM	Run entropy	0.929 (0.919 - 0.939)
Wavelet	HHH	GLRLM	Run length non uniformity	0.98 (0.977 - 0.983)

Feature identifier *				
Pre-processing		Family	Feature name	ICC (95% CI)
Wavelet	HHH	GLRLM	Run length non uniformity normalized	0.916 (0.903 - 0.928)
Wavelet	HHH	GLRLM	Run percentage	0.921 (0.909 - 0.932)
Wavelet	HHH	GLRLM	Run variance	0.931 (0.921 - 0.941)
Wavelet	HHH	GLRLM	Short run emphasis	0.922 (0.911 - 0.933)
Wavelet	HHH	GLRLM	Short run high gray level emphasis	0.884 (0.867 - 0.899)
Wavelet	HHH	GLRLM	Short run low gray level emphasis	0.853 (0.831 - 0.872)
Wavelet	HHH	GLSZM	Gray level non uniformity	0.982 (0.979 - 0.984)
Wavelet	HHH	GLSZM	Gray level non uniformity normalized	0.87 (0.851 - 0.887)
Wavelet	HHH	GLSZM	Gray level variance	0.895 (0.879 - 0.909)
Wavelet	HHH	GLSZM	High gray level zone emphasis	0.889 (0.873 - 0.904)
Wavelet	HHH	GLSZM	Large area emphasis	0.745 (0.713 - 0.776)
Wavelet	HHH	GLSZM	Large area high gray level emphasis	0.952 (0.945 - 0.959)
Wavelet	HHH	GLSZM	Large area low gray level emphasis	0.614 (0.572 - 0.656)
Wavelet	HHH	GLSZM	Low gray level zone emphasis	0.867 (0.847 - 0.884)
Wavelet	HHH	GLSZM	Size zone non uniformity	0.942 (0.933 - 0.95)
Wavelet	HHH	GLSZM	Size zone non uniformity normalized	0.761 (0.73 - 0.791)
Wavelet	HHH	GLSZM	Small area emphasis	0.822 (0.797 - 0.845)
Wavelet	HHH	GLSZM	Small area high gray level emphasis	0.881 (0.863 - 0.897)
Wavelet	HHH	GLSZM	Small area low gray level emphasis	0.64 (0.599 - 0.68)
Wavelet	HHH	GLSZM	Zone entropy	0.914 (0.901 - 0.926)
Wavelet	HHH	GLSZM	Zone percentage	0.889 (0.873 - 0.904)
Wavelet	HHH	GLSZM	Zone variance	0.754 (0.722 - 0.784)
Wavelet	HHH	NGTDM	Busyness	0.607 (0.564 - 0.65)
Wavelet	HHH	NGTDM	Coarseness	0.985 (0.982 - 0.987)
Wavelet	HHH	NGTDM	Complexity	0.843 (0.82 - 0.863)
Wavelet	HHH	NGTDM	Contrast	0.832 (0.808 - 0.854)
Wavelet	HHH	NGTDM	Strength	0.872 (0.854 - 0.89)
Wavelet	LLL	First-order	10th percentile	0.5 (0.452 - 0.549)
Wavelet	LLL	First-order	90th percentile	0.787 (0.758 - 0.814)
Wavelet	LLL	First-order	Energy	0.904 (0.89 - 0.917)
Wavelet	LLL	First-order	Entropy	0.991 (0.99 - 0.993)
Wavelet	LLL	First-order	Interquartile range	0.887 (0.871 - 0.903)
Wavelet	LLL	First-order	Kurtosis	1 (1 - 1)
Wavelet	LLL	First-order	Maximum	0.802 (0.775 - 0.827)
Wavelet	LLL	First-order	Mean absolute deviation	0.877 (0.859 - 0.894)
Wavelet	LLL	First-order	Mean	0.709 (0.673 - 0.743)
Wavelet	LLL	First-order	Median	0.7 (0.663 - 0.735)
Wavelet	LLL	First-order	Minimum	0.442 (0.392 - 0.492)
Wavelet	LLL	First-order	Range	0.862 (0.842 - 0.88)
Wavelet	LLL	First-order	Robust mean absolute deviation	0.884 (0.867 - 0.9)
Wavelet	LLL	First-order	Root mean squared	0.734 (0.7 - 0.766)
Wavelet	LLL	First-order	Skewness	1 (1 - 1)
Wavelet	LLL	First-order	Total energy	0.904 (0.89 - 0.917)
Wavelet	LLL	First-order	Uniformity	0.992 (0.99 - 0.993)
Wavelet	LLL	First-order	Variance	0.824 (0.799 - 0.846)
Wavelet	LLL	GLCM	Autocorrelation	0.809 (0.783 - 0.833)
Wavelet	LLL	GLCM	Cluster prominence	0.702 (0.666 - 0.737)
Wavelet	LLL	GLCM	Cluster shade	0.78 (0.75 - 0.807)
Wavelet	LLL	GLCM	Cluster tendency	0.831 (0.807 - 0.853)
Wavelet	LLL	GLCM	Contrast	0.772 (0.742 - 0.8)
Wavelet	LLL	GLCM	Correlation	1 (1 - 1)
Wavelet	LLL	GLCM	Difference average	0.829 (0.805 - 0.851)
Wavelet	LLL	GLCM	Difference entropy	0.985 (0.983 - 0.988)
Wavelet	LLL	GLCM	Difference variance	0.781 (0.752 - 0.808)
Wavelet	LLL	GLCM	Inverse difference	0.874 (0.855 - 0.891)
Wavelet	LLL	GLCM	Inverse difference moment	0.859 (0.839 - 0.878)
Wavelet	LLL	GLCM	Inverse difference moment normalized	1 (1 - 1)
Wavelet	LLL	GLCM	Inverse difference normalized	1 (1 - 1)
Wavelet	LLL	GLCM	Informational measure of correlation 1	0.9 (0.885 - 0.914)
Wavelet	LLL	GLCM	Informational measure of correlation 2	0.952 (0.944 - 0.958)
Wavelet	LLL	GLCM	Inverse variance	0.833 (0.809 - 0.855)
Wavelet	LLL	GLCM	Joint average	0.857 (0.836 - 0.876)
Wavelet	LLL	GLCM	Joint energy	1 (1 - 1)
Wavelet	LLL	GLCM	Joint entropy	1 (1 - 1)
Wavelet	LLL	GLCM	Maximal correlation coefficient	0.823 (0.798 - 0.846)
Wavelet	LLL	GLCM	Maximum probability	0.996 (0.995 - 0.996)
Wavelet	LLL	GLCM	Sum average	0.857 (0.836 - 0.876)
Wavelet	LLL	GLCM	Sum entropy	0.998 (0.998 - 0.998)
Wavelet	LLL	GLCM	Sum squares	0.822 (0.798 - 0.845)
Wavelet	LLL	GLDM	Dependence entropy	0.994 (0.993 - 0.994)
Wavelet	LLL	GLDM	Dependence non uniformity	0.999 (0.999 - 0.999)
Wavelet	LLL	GLDM	Dependence non uniformity normalized	0.756 (0.724 - 0.785)
Wavelet	LLL	GLDM	Dependence variance	0.714 (0.679 - 0.748)
Wavelet	LLL	GLDM	Gray level non uniformity	0.936 (0.926 - 0.945)
Wavelet	LLL	GLDM	Gray level variance	0.824 (0.799 - 0.846)
Wavelet	LLL	GLDM	High gray level emphasis	0.812 (0.786 - 0.836)
Wavelet	LLL	GLDM	Large dependence emphasis	0.741 (0.708 - 0.772)
Wavelet	LLL	GLDM	Large dependence high gray level emphasis	0.818 (0.793 - 0.842)
Wavelet	LLL	GLDM	Large dependence low gray level emphasis	0.971 (0.967 - 0.975)
Wavelet	LLL	GLDM	Low gray level emphasis	0.983 (0.98 - 0.985)
Wavelet	LLL	GLDM	Small dependence emphasis	0.756 (0.724 - 0.786)
Wavelet	LLL	GLDM	Small dependence high gray level emphasis	0.81 (0.784 - 0.834)
Wavelet	LLL	GLDM	Small dependence low gray level emphasis	0.982 (0.979 - 0.985)
Wavelet	LLL	GLRLM	Gray level non uniformity	0.936 (0.926 - 0.945)
Wavelet	LLL	GLRLM	Gray level non uniformity normalized	0.992 (0.99 - 0.993)
Wavelet	LLL	GLRLM	Gray level variance	0.824 (0.799 - 0.846)
Wavelet	LLL	GLRLM	High gray level run emphasis	0.812 (0.786 - 0.836)
Wavelet	LLL	GLRLM	Long run emphasis	0.75 (0.718 - 0.781)
Wavelet	LLL	GLRLM	Long run high gray level emphasis	0.812 (0.786 - 0.836)
Wavelet	LLL	GLRLM	Long run low gray level emphasis	0.983 (0.98 - 0.985)
Wavelet	LLL	GLRLM	Low gray level run emphasis	0.983 (0.98 - 0.985)
Wavelet	LLL	GLRLM	Run entropy	0.991 (0.99 - 0.993)
Wavelet	LLL	GLRLM	Run length non uniformity	1 (1 - 1)
Wavelet	LLL	GLRLM	Run length non uniformity normalized	0.753 (0.721 - 0.783)
Wavelet	LLL	GLRLM	Run percentage	0.752 (0.72 - 0.782)
Wavelet	LLL	GLRLM	Run variance	0.746 (0.714 - 0.777)
Wavelet	LLL	GLRLM	Short run emphasis	0.752 (0.72 - 0.783)
Wavelet	LLL	GLRLM	Short run high gray level emphasis	0.812 (0.786 - 0.836)
Wavelet	LLL	GLRLM	Short run low gray level emphasis	0.983 (0.98 - 0.985)
Wavelet	LLL	GLSZM	Gray level non uniformity	0.941 (0.932 - 0.95)
Wavelet	LLL	GLSZM	Gray level non uniformity normalized	0.992 (0.991 - 0.993)
Wavelet	LLL	GLSZM	Gray level variance	0.823 (0.799 - 0.846)
Wavelet	LLL	GLSZM	High gray level zone emphasis	0.811 (0.785 - 0.835)

Feature identifier *				
Pre-processing		Family	Feature name	ICC (95% CI)
Wavelet	LLL	GLSZM	Large area emphasis	0.74 (0.707 - 0.772)
Wavelet	LLL	GLSZM	Large area high gray level emphasis	0.815 (0.789 - 0.839)
Wavelet	LLL	GLSZM	Large area low gray level emphasis	0.979 (0.976 - 0.982)
Wavelet	LLL	GLSZM	Low gray level zone emphasis	0.982 (0.979 - 0.985)
Wavelet	LLL	GLSZM	Size zone non uniformity	0.999 (0.999 - 1)
Wavelet	LLL	GLSZM	Size zone non uniformity normalized	0.75 (0.718 - 0.781)
Wavelet	LLL	GLSZM	Small area emphasis	0.75 (0.718 - 0.781)
Wavelet	LLL	GLSZM	Small area high gray level emphasis	0.81 (0.784 - 0.835)
Wavelet	LLL	GLSZM	Small area low gray level emphasis	0.982 (0.979 - 0.985)
Wavelet	LLL	GLSZM	Zone entropy	0.993 (0.992 - 0.994)
Wavelet	LLL	GLSZM	Zone percentage	0.756 (0.724 - 0.786)

Feature identifier *				
Pre-processing		Family	Feature name	ICC (95% CI)
Wavelet	LLL	GLSZM	Zone variance	0.717 (0.681 - 0.75)
Wavelet	LLL	NGTDM	Busyness	0.981 (0.978 - 0.984)
Wavelet	LLL	NGTDM	Coarseness	0.927 (0.915 - 0.937)
Wavelet	LLL	NGTDM	Complexity	0.862 (0.842 - 0.88)
Wavelet	LLL	NGTDM	Contrast	0.682 (0.644 - 0.719)
Wavelet	LLL	NGTDM	Strength	0.882 (0.864 - 0.898)

* Feature identifiers are composed of a pre-processing specification (left column: type of pre-processing, i.e. wavelet- or LoG-filtering or original; right column: 3-letter directional specification of wavelet (*6,13*), or LoG sigma setting), and the feature family and feature name (supplemental table 2).

To investigate whether PET intensity normalization affects radiomic feature values, we utilized the entire patient cohort and extracted the full set of radiomic features after applying four different PET normalization techniques ("SUV", "none", "lentiform nucleus", "cerebellum"). We then calculated a two-way mixed effects absolute agreement single rater/measurement ICC for each radiomic feature to quantify its reproducibility across PET normalization techniques. Note that radiomic features were standardized prior to ICC calculation.

CI, confidence interval; GLCM, Gray Level Cooccurrence Matrix; GLDM, Gray Level Dependence Matrix; GLRLM, Gray Level Run Length Matrix; GLSZM, Gray Level Size Zone Matrix; ICC, intraclass correlation coefficient; LoG, Laplacian of Gaussian; NGTDM, Neighboring Gray Tone Difference Matrix; PET, positron emission tomography, SUV; standardized uptake value.

Supplemental table 6 Categorization of radiomic feature reproducibility across PET normalization techniques

Supplemental table 6.1 Breakdown of original and derived image features

	Reproducibility category				
n features (%)	**Perfect** ICC = 1	**Nearly perfect** 1 > ICC ≥ 0.999	**High degree** 0.999 > ICC ≥ 0.90	**Medium degree** 0.90 > ICC ≥ 0.75	**Low degree** ICC < 0.75
Original image	14 (13.1 %)*	4 (3.7 %)	23 (21.5 %)	54 (50.5 %)	12 (11.2 %)
LoG image (sigma = 3 mm)	0 (0 %)	3 (3.2 %)	26 (28 %)	58 (62.4 %)	6 (6.5 %)
LoG image (sigma = 6 mm)	0 (0 %)	4 (4.3 %)	24 (25.8 %)	58 (62.4 %)	7 (7.5 %)
Wavelet decomposition (LLH)	0 (0 %)	6 (6.5 %)	27 (29 %)	54 (58.1 %)	6 (6.5 %)
Wavelet decomposition (LHL)	0 (0 %)	6 (6.5 %)	27 (29 %)	54 (58.1 %)	6 (6.5 %)
Wavelet decomposition (HLL)	0 (0 %)	6 (6.5 %)	27 (29 %)	56 (60.2 %)	4 (4.3 %)
Wavelet decomposition (HHL)	0 (0 %)	2 (2.2 %)	26 (28 %)	62 (66.7 %)	3 (3.2 %)
Wavelet decomposition (HLH)	0 (0 %)	2 (2.2 %)	18 (19.4 %)	66 (71 %)	7 (7.5 %)
Wavelet decomposition (LHH)	0 (0 %)	2 (2.2 %)	21 (22.6 %)	65 (69.9 %)	5 (5.4 %)
Wavelet decomposition (LLL)	0 (0 %)	10 (10.8 %)	28 (30.1 %)	43 (46.2 %)	12 (12.9 %)
Wavelet decomposition (HHH)	0 (0 %)	2 (2.2 %)	48 (51.6 %)	38 (40.9 %)	5 (5.4 %)
All	14 (1.4 %)*	47 (4.5 %)†	295 (28.4 %)	608 (58.6 %)	73 (7 %)

* Only and all shape features, which are extracted from original images only.
† Thereof, n=11 are "Skewness" features extracted from the n=11 different image types, n=11 were "Kurtosis" features, n=7 "Correlation" features, and n=6 "Run Length Non Uniformity" features.

Supplemental table 6.2 Breakdown of radiomic feature families

	Reproducibility category				
n features (%)	**Perfect** ICC = 1	**Nearly perfect** 1 > ICC ≥ 0.999	**High degree** 0.999 > ICC ≥ 0.90	**Medium degree** 0.90 > ICC ≥ 0.75	**Low degree** ICC < 0.75
Shape	14 (100 %)	0 (0 %)	0 (0 %)	0 (0 %)	0 (0 %)
First-order	0 (0 %)	22 (11.1 %)*	37 (18.7 %)	129 (65.2 %)	10 (5.1 %)
GLCM	0 (0 %)	17 (6.4 %)	82 (31.1 %)	150 (56.8 %)	15 (5.7 %)
GLSZM	0 (0 %)	1 (0.6 %)	50 (28.4 %)	95 (54 %)	30 (17 %)
GLRLM	0 (0 %)	6 (3.4 %)	56 (31.8 %)	113 (64.2 %)	1 (0.6 %)
NGTDM	0 (0 %)	0 (0 %)	13 (23.6 %)	35 (63.6 %)	7 (12.7 %)
GLDM	0 (0 %)	1 (0.6 %)	57 (37 %)	86 (55.8 %)	10 (6.5 %)
All	14 (1.4 %)	47 (4.5 %)	295 (28.4 %)	608 (58.6 %)	73 (7 %)

* Only and all “Skewness” and “Kurtosis” features extracted from n=11 different image types.

To investigate whether PET intensity normalization affects radiomic feature values, we utilized the entire patient cohort and extracted the full set of radiomic features after applying four different PET normalization techniques (“SUV”, “none”, “lentiform nucleus”, “cerebellum”). We then calculated a two-way mixed effects absolute agreement single rater/measurement ICC for each radiomic feature to quantify its reproducibility across PET normalization techniques. Note that radiomic features were standardized prior to ICC calculation.

GLCM, Gray Level Cooccurrence Matrix; GLDM, Gray Level Dependence Matrix; GLRLM, Gray Level Run Length Matrix; GLSZM, Gray Level Size Zone Matrix; ICC, intraclass correlation coefficient; LoG, Laplacian of Gaussian; NGTDM, Neighboring Gray Tone Difference Matrix.

Supplemental table 7 Univariate logistic regression

Supplemental table 7.1 Breakdown of original and derived image features

n/n of significant features before/after p-value adjustment * for multiple testing	PET normalization method			
	SUV	**None (raw intensities)**	**Reference tissue: lentiform nucleus**	**Reference tissue: cerebellum**
Original image (n=107 features)	57/54	90/89	94/92	82/80
LoG image (sigma = 3 mm; n=93 features)	57/56	76/76	79/78	73/69
LoG image (sigma = 6 mm; n=93 features)	54/53	74/74	76/75	70/69
Wavelet decomposition (LLH; n=93 features)	67/62	83/79	82/80	80/77
Wavelet decomposition (LHL; n=93 features)	54/49	73/71	79/79	70/69
Wavelet decomposition (HLL; n=93 features)	66/62	81/77	80/78	78/73
Wavelet decomposition (HHL; n=93 features)	62/62	77/77	77/76	73/72
Wavelet decomposition (HLH; n=93 features)	60/57	78/78	82/81	76/75
Wavelet decomposition (LHH; n=93 features)	61/55	77/77	78/78	75/73
Wavelet decomposition (LLL; n=93 features)	55/54	75/73	85/84	71/70
Wavelet decomposition (HHH; n=93 features)	30/27	73/72	65/64	61/58
All (n=1037 features)	623/591	857/843	877/865	809/785

* Adjustment by Benjamini and Hochberg's method.

Supplemental table 7.2 Breakdown of radiomic feature families

n/n of significant features before/after p-value adjustment * for multiple testing	PET normalization method			
	SUV	**None (raw intensities)**	**Reference tissue: lentiform nucleus**	**Reference tissue: cerebellum**
Shape (n=14 features)	12/12	12/12	12/12	12/12
First-order (n=198 features)	126/120	171/170	173/173	160/160
GLCM (n=264 features)	176/171	223/220	218/215	215/210
GLSZM (n=176 features)	97/91	135/133	141/140	130/125
GLRLM (n=176 features)	103/93	149/145	160/156	138/130
NGTDM (n=55 features)	24/24	40/38	43/42	36/34
GLDM (n=154 features)	85/80	127/125	130/127	118/114
All (n=1037 features)	623/591	857/843	877/865	809/785

* Adjustment by Benjamini and Hochberg's method.

Summary of the n/n of significant features before/after p-value adjustment for multiple testing from a series of logistic regressions with HPV as the dependent variable and each radiomic feature from each intensity-normalized PET image type as the independent variable. Note that radiomic features were standardized prior to analysis.

GLCM, Gray Level Cooccurrence Matrix; GLDM, Gray Level Dependence Matrix; GLRLM, Gray Level Run Length Matrix; GLSZM, Gray Level Size Zone Matrix; HPV, human papilloma virus; LoG, Laplacian of Gaussian; NGTDM, Neighboring Gray Tone Difference Matrix; PET, positron emission tomography; SUV, standardized uptake value.

Supplemental table 8 XGBoost feature importance

Supplemental table 8.1 XGBoost classifier using SUV-normalized PET features

Feature identifier *				Feature Importance †	
Pre-processing		**Family**	**Feature name**	**Rank**	**Score**
Wavelet	HLL	GLSZM	Large area high gray level emphasis	1	0.781
Wavelet	LLL	GLCM	Maximal correlation coefficient	2	0.219

Supplemental table 8.2 XGBoost classifier using raw PET (no normalization) features

Feature identifier *				Feature Importance †	
Pre-processing		**Family**	**Feature name**	**Rank**	**Score**
Wavelet	HLL	GLCM	Difference variance	1	0.276
Wavelet	HLL	GLCM	Sum average	2	0.228
LoG	3 mm	GLSZM	Large area high gray level emphasis	3	0.087
Wavelet	LHH	First-order	Median	4	0.054
Original	n/a	Shape	Sphericity	5	0.051
Wavelet	LLH	GLCM	Cluster shade	6	0.042
Wavelet	LHL	GLCM	Contrast	7	0.040
Original	n/a	First-order	Minimum	8	0.035
Wavelet	LLH	GLCM	Informational Measure of Correlation 2	9	0.029
Wavelet	LHL	First-order	Kurtosis	10	0.027
Wavelet	HLL	First-order	Kurtosis	11	0.026
Wavelet	HHH	GLSZM	Zone variance	12	0.025
Wavelet	HLL	GLCM	Cluster shade	13	0.021
Wavelet	LHL	GLCM	Cluster shade	14	0.021
Wavelet	LLH	First-order	Skewness	15	0.013
Wavelet	HLH	GLDM	Large dependence low gray level emphasis	16	0.009
Wavelet	HLH	GLCM	Correlation	17	0.006
LoG	6 mm	First-order	Kurtosis	18	0.006
Wavelet	HLL	GLSZM	Zone variance	19	0.006

Supplemental table 8.3 XGBoost classifier using features from PET normalized to lentiform nucleus

Feature identifier *				Feature Importance †	
Pre-processing		**Family**	**Feature name**	**Rank**	**Score**
Wavelet	HLL	GLCM	Difference Variance	1	0.2709
Wavelet	LLH	First-order	90th percentile	2	0.103879
Original	n/a	GLDM	Large dependence low gray level emphasis	3	0.087817
Original	n/a	First-order	Minimum	4	0.087013

Original	n/a	Shape	Sphericity	5	0.060994
Wavelet	LLL	GLCM	Cluster shade	6	0.055667
Wavelet	LLL	First-order	Kurtosis	7	0.050477
Wavelet	HHL	GLCM	Contrast	8	0.044468
Wavelet	HHH	GLSZM	Small area low gray level emphasis	9	0.039314
Wavelet	HLL	GLCM	Cluster shade	10	0.032551
Wavelet	LHL	GLCM	Cluster shade	11	0.03148
Wavelet	HLL	First-order	Kurtosis	12	0.026434
Wavelet	HHH	First-order	Median	13	0.019049
Wavelet	LLH	GLCM	Cluster shade	14	0.018368
Wavelet	HHL	NGTDM	Contrast	15	0.01729
Wavelet	HHH	GLSZM	Size zone non uniformity normalized	16	0.01641
Wavelet	HLH	GLSZM	Large area low gray level emphasis	17	0.012899
Wavelet	LLH	First-order	Kurtosis	18	0.009956
Original	n/a	Shape	Maximum 2D diameter slice	19	0.009784
Wavelet	HHH	First-order	Skewness	20	0.005252

Supplemental table 8.4 XGBoost classifier using features from PET normalized to cerebellum

Feature identifier *				**Feature Importance †**	
Pre-processing		**Family**	**Feature name**	**Rank**	**Score**
Wavelet	HLL	GLDM	Large dependence high gray level emphasis	1	0.193
Wavelet	HLL	GLCM	Difference variance	2	0.168
Wavelet	LHL	GLCM	Cluster shade	3	0.092
Original	n/a	Shape	Sphericity	4	0.071
Wavelet	LHL	NGTDM	Contrast	5	0.070
Wavelet	LLH	GLCM	Cluster shade	6	0.068
Wavelet	HHH	GLSZM	Size zone non uniformity normalized	7	0.058
Original	n/a	GLCM	Cluster shade	8	0.056
Original	n/a	First-order	Skewness	9	0.043
Wavelet	LHH	First-order	Median	10	0.039
Original	n/a	Shape	Maximum 2D diameter slice	11	0.032
Wavelet	LLH	First-order	90th percentile	12	0.018
Wavelet	LHH	GLSZM	Large area low gray level emphasis	13	0.018
Wavelet	HHH	First-order	Skewness	14	0.017
Original	n/a	First-order	Minimum	15	0.017
Wavelet	LLH	First-order	Kurtosis	16	0.016
Wavelet	HHL	GLCM	Cluster prominence	17	0.011
Wavelet	LHL	GLCM	Difference variance	18	0.011

* Feature identifiers are composed of a pre-processing specification (left column: type of pre-processing, i.e. wavelet- or LoG-filtering or original; right column: 3-letter directional specification of wavelet (*6,13*), or LoG sigma setting), and the feature family and feature name (supplemental table 2)
† Features' "gain" value determined by the "xgb.importance" function ("xgboost" package version 1.6.0.1 for R (*9*)).

Four XGBoost classifiers, each utilizing an MRMR-selected feature subset from a different intensity-normalized image type, were trained and optimized in the training cohort. The table depicts final models' feature importance scores and ranks. Note that the number of radiomic features included in each final model was optimized using Bayesian optimization.

GLCM, Gray Level Cooccurrence Matrix; GLDM, Gray Level Dependence Matrix; GLRLM, Gray Level Run Length Matrix; GLSZM, Gray Level Size Zone Matrix; LoG, Laplacian of Gaussian; MRMR, minimum redundancy maximum relevance feature selection; NGTDM, Neighboring Gray Tone Difference Matrix; PET, positron emission tomography; SUV, standardized uptake value; XGBoost, extreme gradient boosting machine learning classifier.

3. Supplemental figures

Supplemental figure 1 Radiomic feature reproducibility across PET normalization techniques

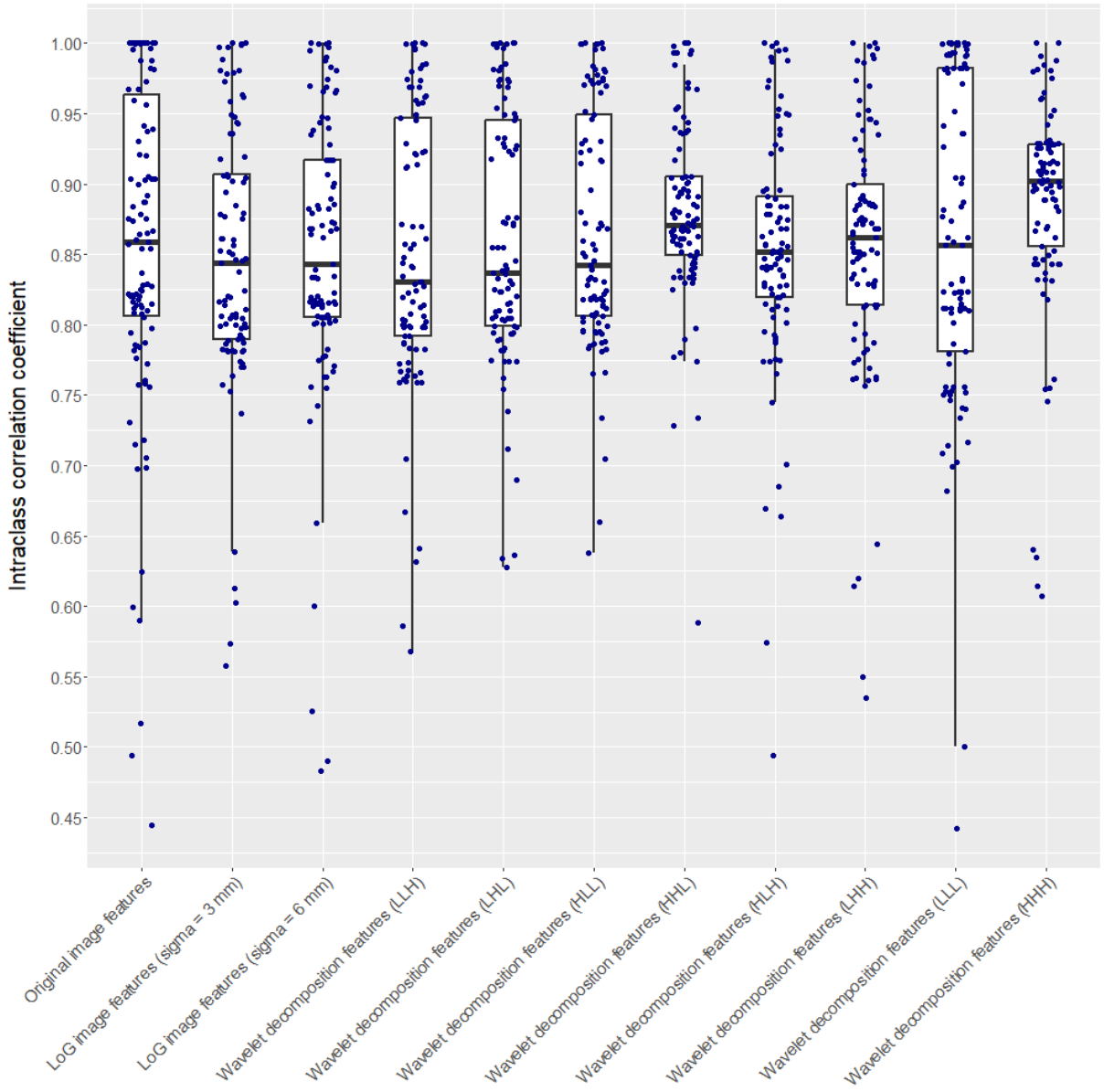

Supplemental figure 1.1 Breakdown of original and derived image features

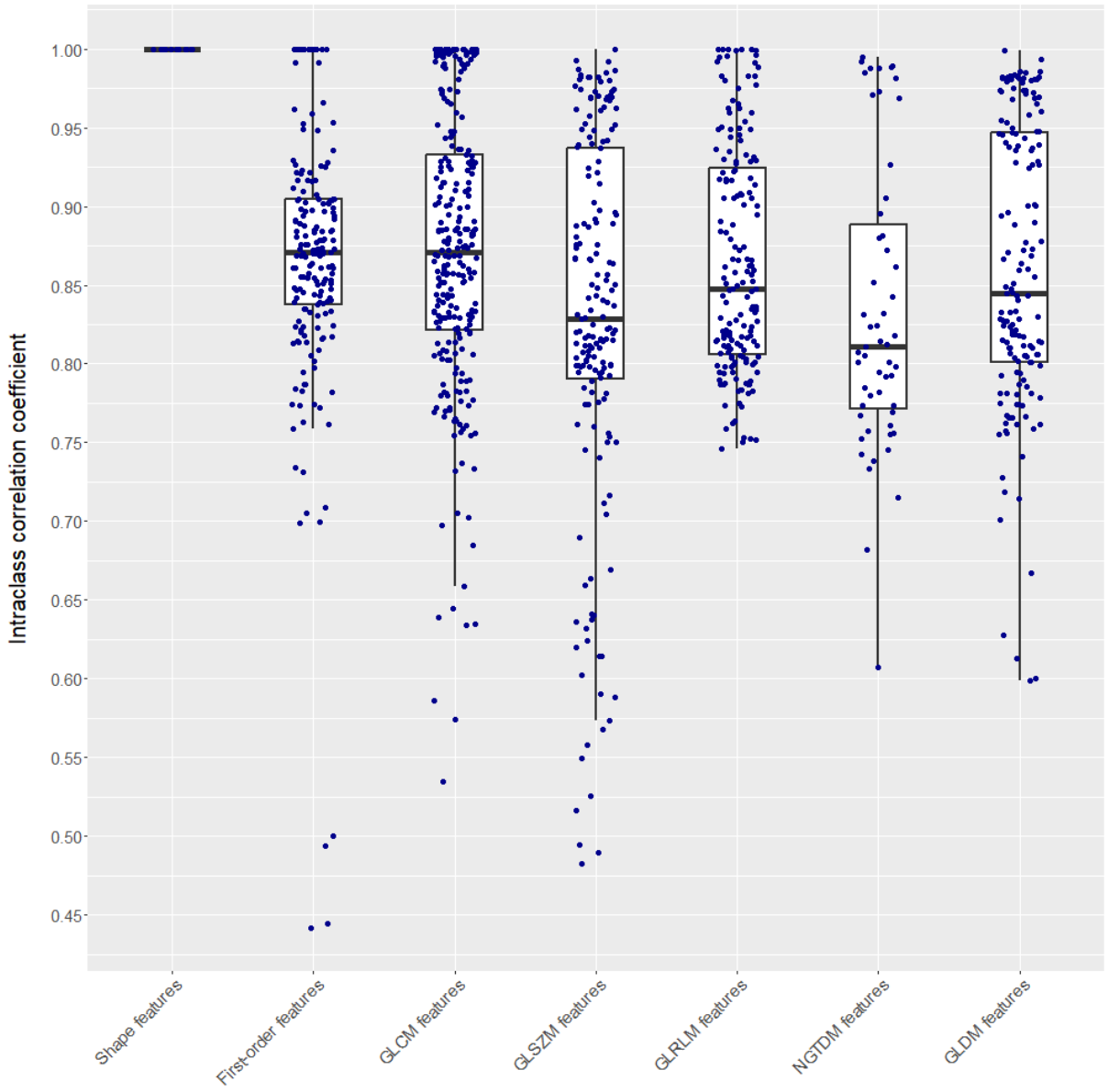

Supplemental figure 1.2 Breakdown of radiomic feature families

Supplemental figure 1 shows box-whisker-plots of ICC scores superimposed with scatter plots (with horizontal jitter applied, i.e. random variation of the horizontal position of each data point reducing overplotting). Note that radiomic features were standardized prior to ICC calculation.

GLCM, Gray Level Cooccurrence Matrix; GLDM, Gray Level Dependence Matrix; GLRLM, Gray Level Run Length Matrix; GLSZM, Gray Level Size Zone Matrix; ICC, intraclass correlation coefficient; LoG, Laplacian of Gaussian; NGTDM, Neighboring Gray Tone Difference Matrix.

Supplemental figure 2 Univariate association analysis

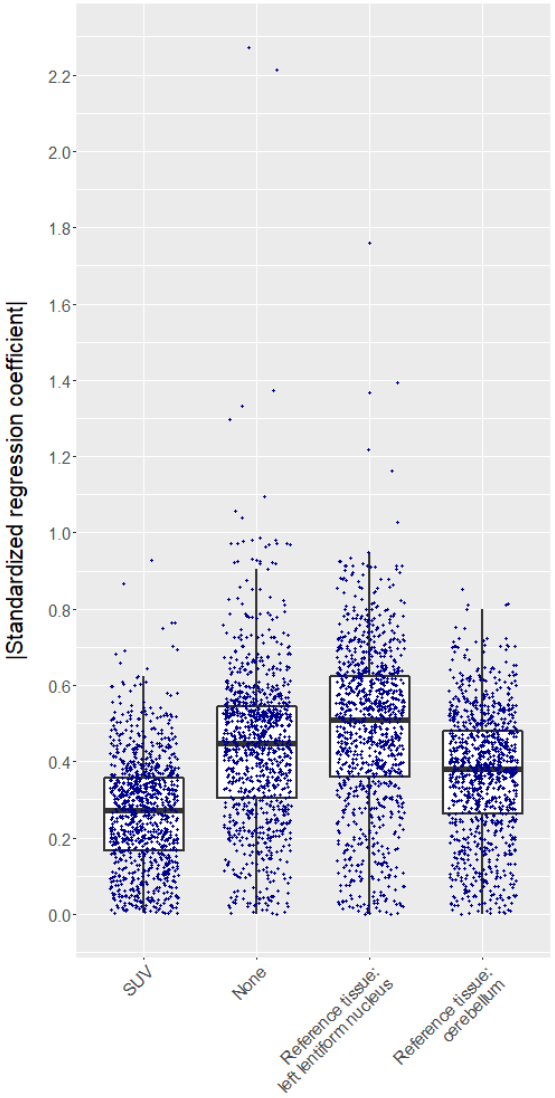

Supplemental figure 2.1 Absolute standardized regression coefficients of all features

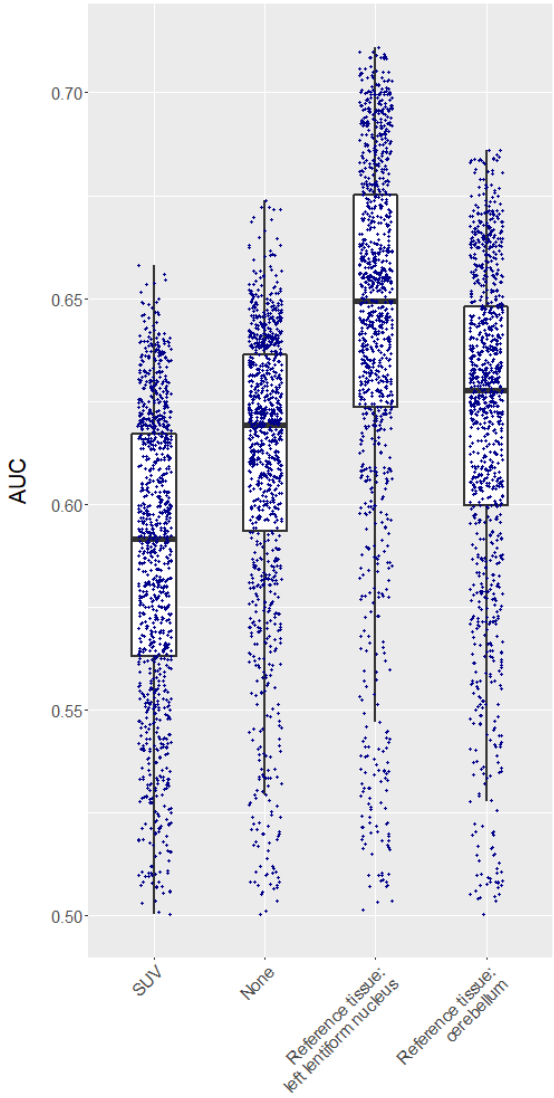

Supplemental figure 2.2 AUC scores of all features

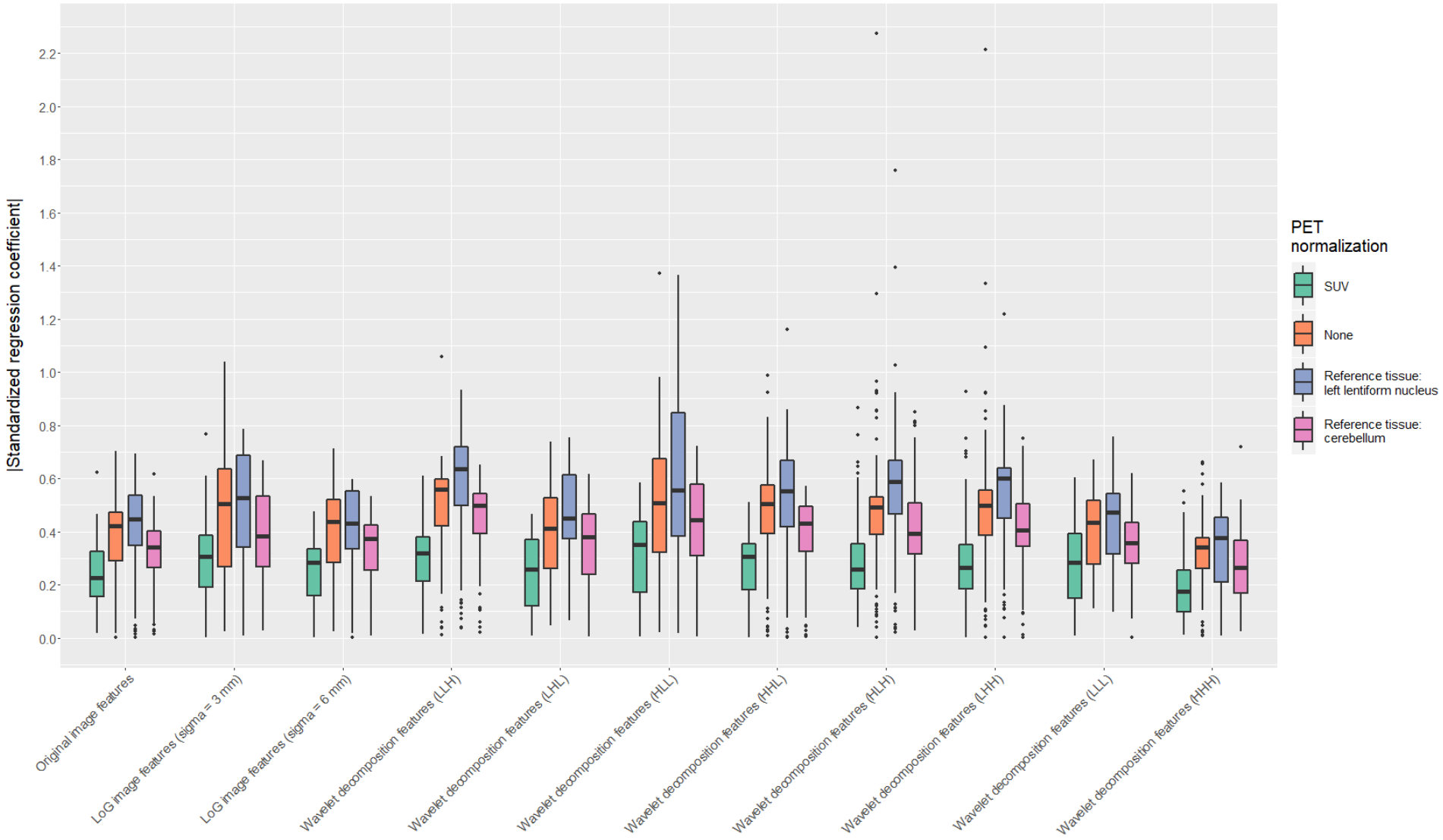

Supplemental figure 2.3 Absolute standardized regression coefficients - breakdown of original and derived image features

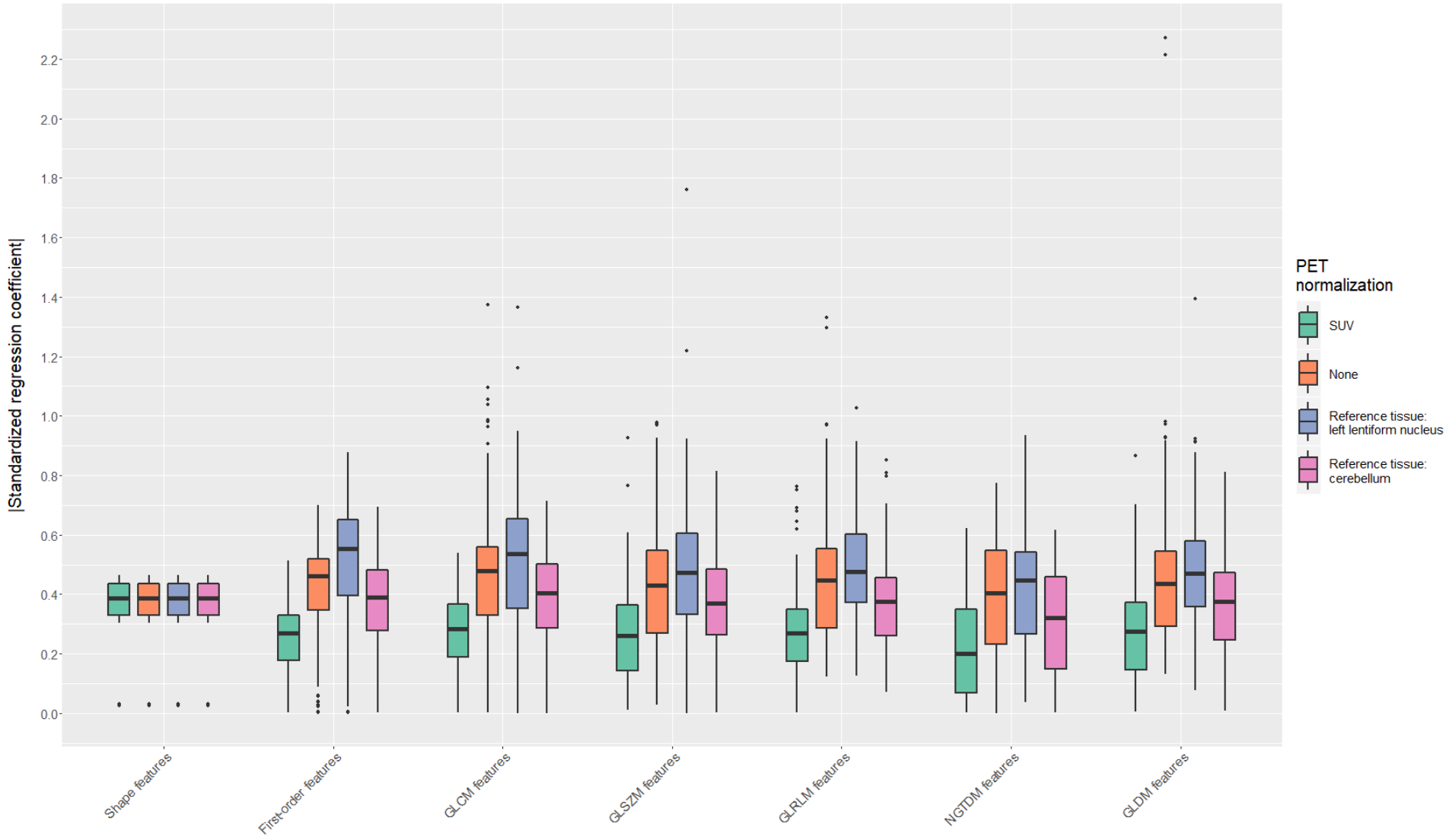

Supplemental figure 2.4 Absolute standardized regression coefficients - breakdown of radiomic feature families

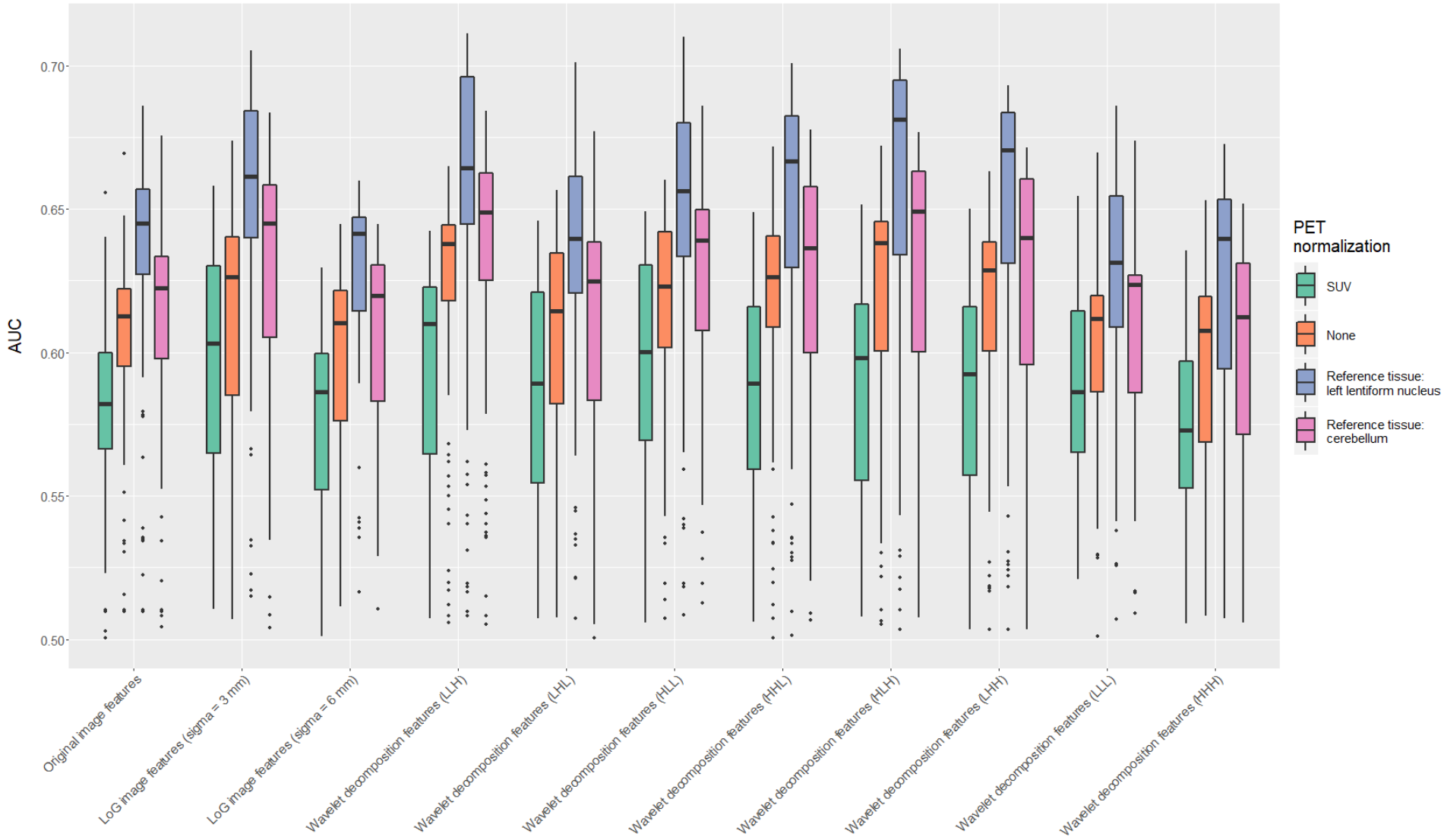

Supplemental figure 2.5 AUC scores - breakdown of original and derived image features

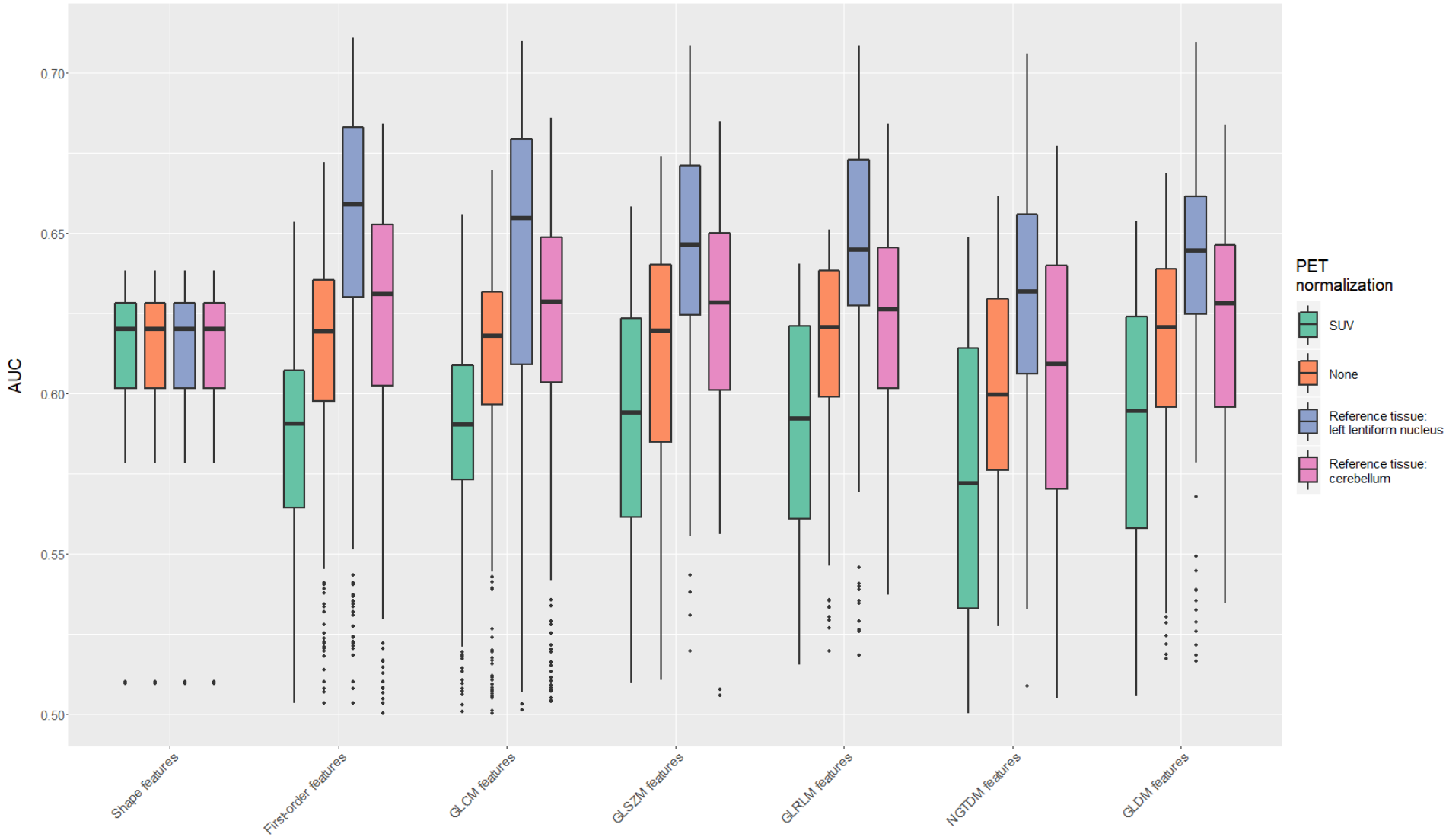

Supplemental figure 2.6 AUC scores - breakdown of radiomic feature families

Supplemental figure 2 shows box-whisker-plots of absolute standardized regression coefficients or AUC scores. In sub-figures 2.1 and 2.2, box-plots are superimposed with scatter plots (with horizontal jitter applied, i.e. random variation of the horizontal position of each data point reducing overplotting). The figure summarizes regression coefficients of a series of logistic regressions with HPV as the dependent variable and each radiomic feature from each intensity-normalized PET image type as the independent variable. The AUC was determined for each feature as an additional measure of univariate association. Note that standardized regression coefficients were converted to absolute values prior to plotting to enable comparability of features with both positive and inverse association with HPV status. Similarly, AUC values<0.5 were substituted with 1-AUC before plotting. Note that this will positively bias the median values, as non-predictive features whose coefficient and AUC may randomly slightly differ from zero and 0.5, respectively, will always contribute to higher median values. Also note that radiomic features were standardized prior to analysis.

AUC, area under the curve; GLCM, Gray Level Cooccurrence Matrix; GLDM, Gray Level Dependence Matrix; GLRLM, Gray Level Run Length Matrix; GLSZM, Gray Level Size Zone Matrix; HPV, human papilloma virus; LoG, Laplacian of Gaussian; NGTDM, Neighboring Gray Tone Difference Matrix; PET, positron emission tomography; SUV, standardized uptake value.

Supplemental figure 3 Juxtaposition of radiomic features' univariate AUC and ICC values

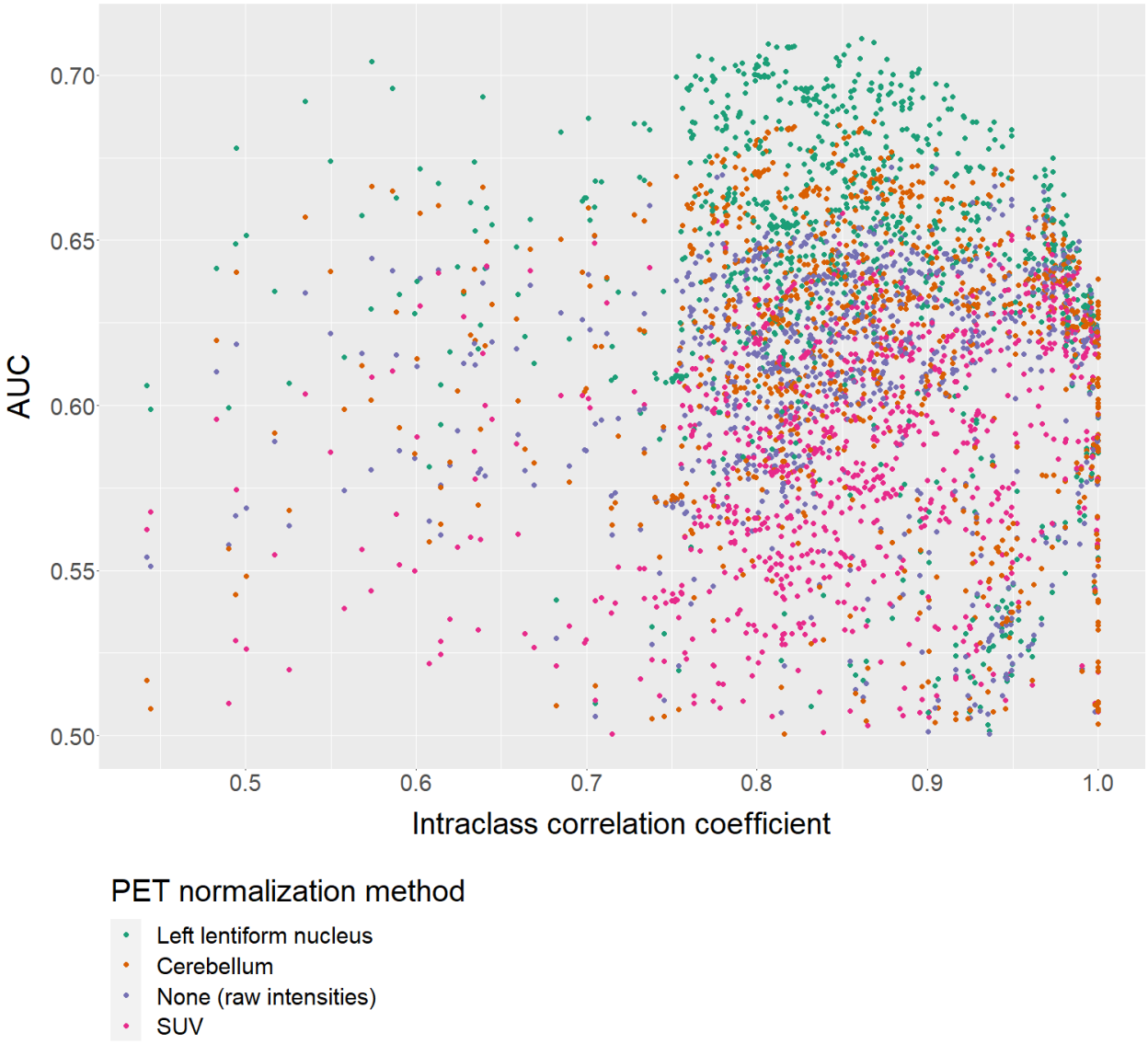

Supplemental figure 3.1 Juxtaposition of AUC and ICC values with color coding of PET normalization methods

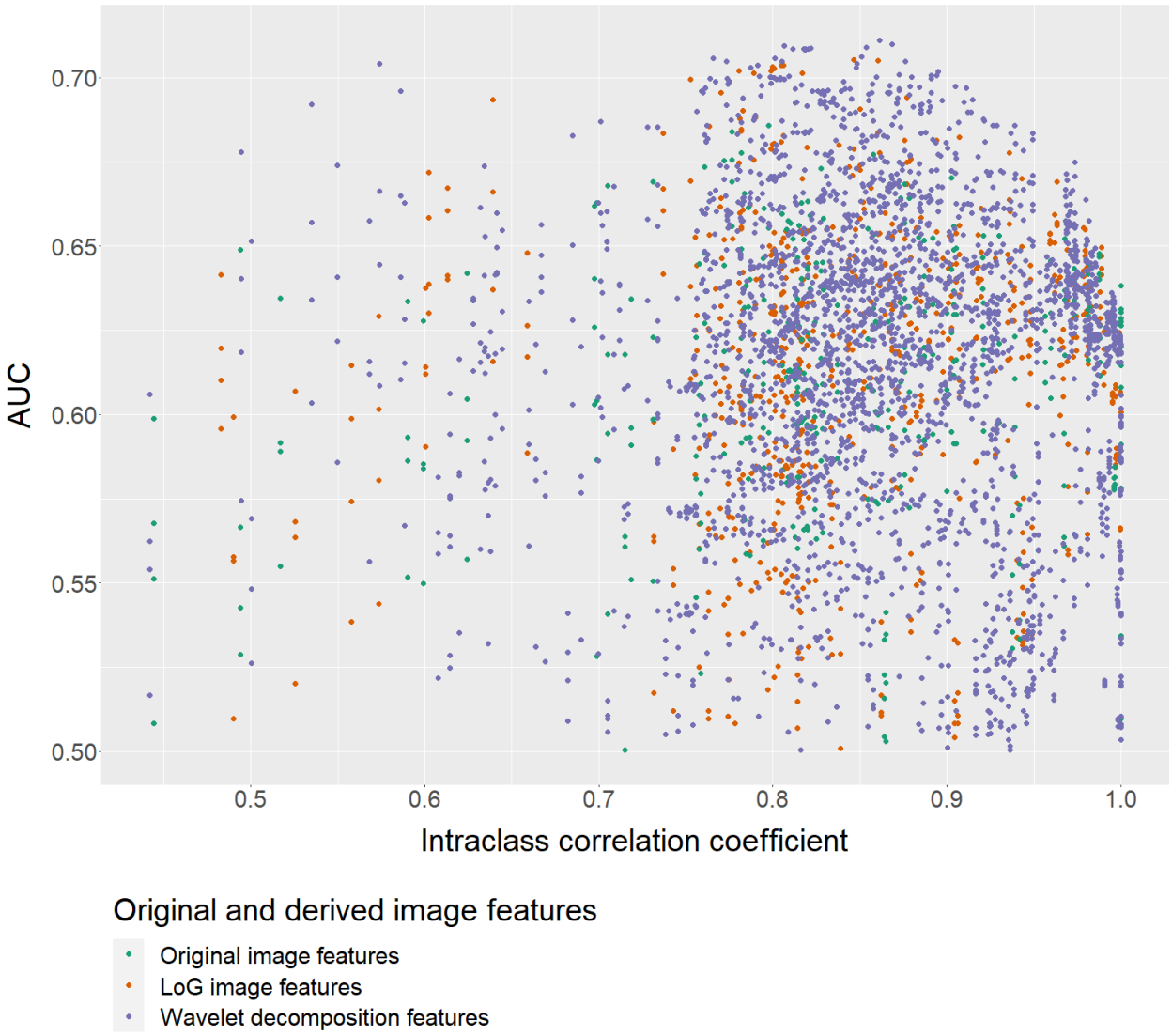

Supplemental figure 3.2 Juxtaposition of AUC and ICC values with color coding of original and derived image features

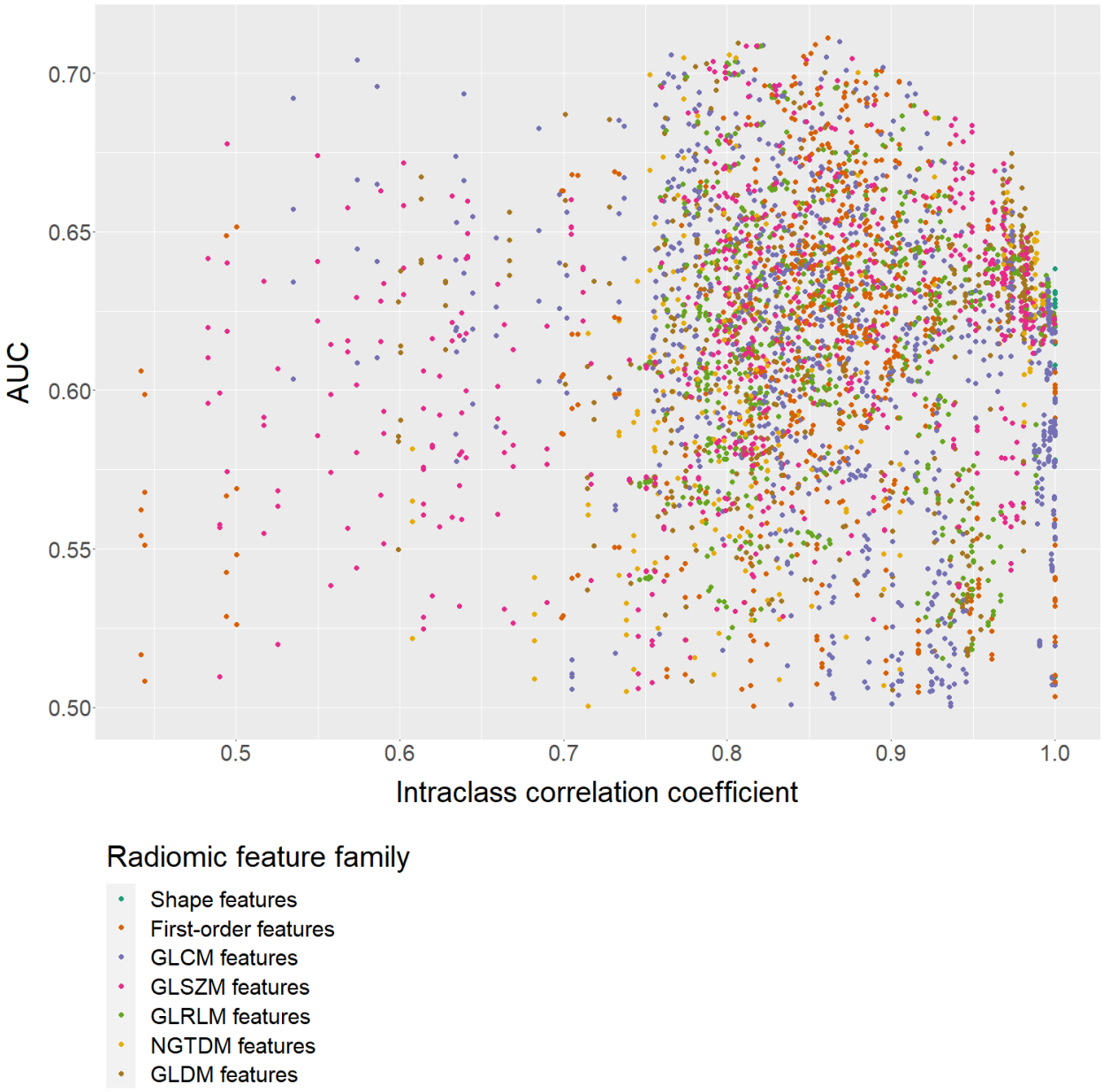

Supplemental figure 3.3 Juxtaposition of AUC and ICC values with color coding of radiomic feature families

Supplemental figure 3 shows a juxtaposition of all radiomic features' univariate AUC (measuring their association with HPV status) and ICC values (measuring their reproducibility across PET normalization methods). All sub-figures depict the full set of n = 14 shape, n = 198 first-order and n = 825 texture features extracted from all four intensity-normalized PET image types, amounting to n = 4148 features in total. Color coding identifies the applied PET normalization method, original and derived image features and radiomic feature family in sub-figure 3.1, 3.2 and 3.3, respectively. Note that AUC values<0.5 were substituted with 1-AUC before plotting to enable comparability of features with both positive and inverse association with HPV status.

AUC, area under the curve; GLCM, Gray Level Cooccurrence Matrix; GLDM, Gray Level Dependence Matrix; GLRLM, Gray Level Run Length Matrix; GLSZM, Gray Level Size Zone Matrix; HPV, human papilloma virus; ICC, intraclass correlation coefficient, LoG, Laplacian of Gaussian; NGTDM, Neighboring Gray Tone Difference Matrix; PET, positron emission tomography; SUV, standardized uptake value.

Supplemental figure 4 Comparison of machine learning classifiers' performance

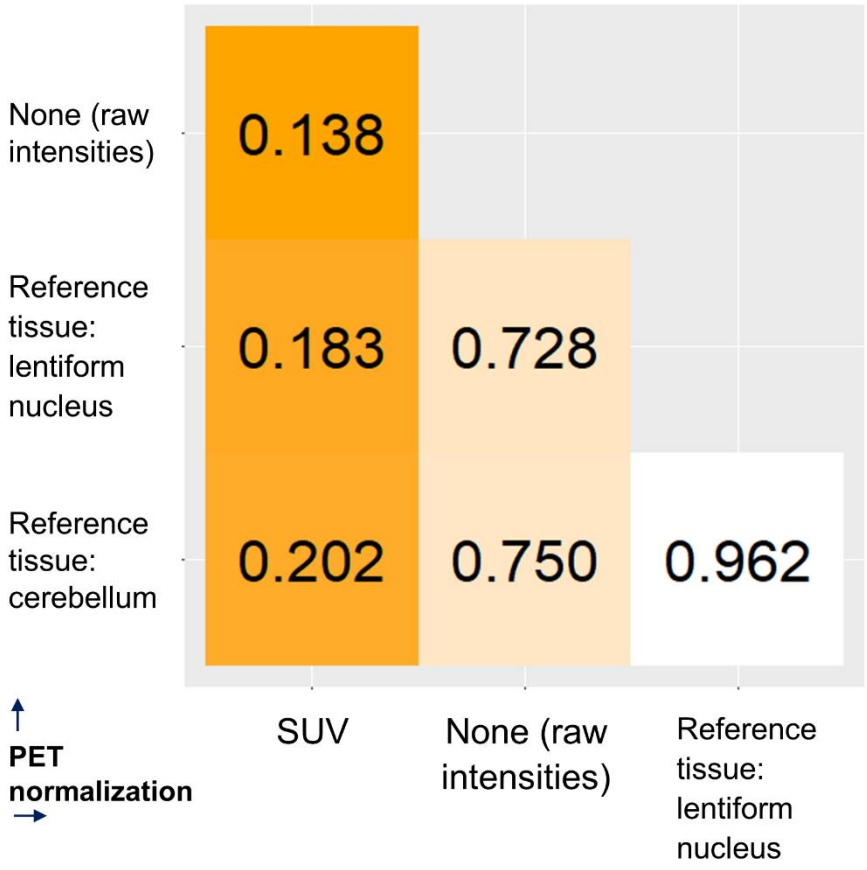

Supplemental figure 4.1 Independent validation dataset

DeLong's test was applied to compare machine learning classifiers' independent validation AUC scores. The heatmap depicts the resulting p values.

AUC, area under the curve; PET, positron emission tomography; SUV, standardized uptake value.

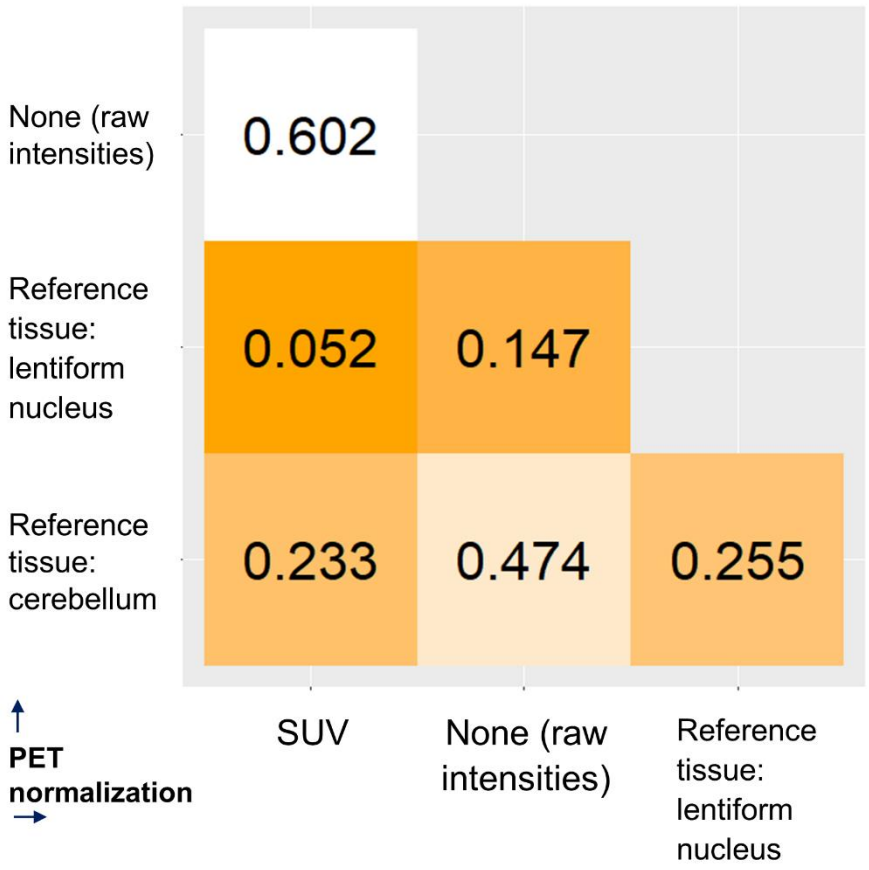

Supplemental figure 4.2 Training dataset

The "corrected repeated k-fold cross validation test" was applied to compare machine learning classifiers' performance in cross-validation in the training dataset. The test was implemented in R following section 3.3 of reference (*14*). The heatmap depicts the resulting two-tailed p values.

AUC, area under the curve; PET, positron emission tomography; SUV, standardized uptake value.

4. References

1. Kinahan P, Clunie D, Boellaard R, et al. Vendor-neutral pseudo-code for SUV calculation. Jun 26th 2018; https://qibawiki.rsna.org/index.php/Standardized_Uptake_Value_(SUV). Accessed Dec 12th, 2022.

2. Britz-Cunningham SH, Millstine JW, Gerbaudo VH. Improved discrimination of benign and malignant lesions on FDG PET/CT, using comparative activity ratios to brain, basal ganglia, or cerebellum. *Clin Nucl Med.* 2008;33:681-687.

3. Helsen N, Van den Wyngaert T, Carp L, et al. Quantification of 18F-fluorodeoxyglucose uptake to detect residual nodal disease in locally advanced head and neck squamous cell carcinoma after chemoradiotherapy: results from the ECLYPS study. *European Journal of Nuclear Medicine and Molecular Imaging.* 2020;47:1075-1082.

4. Haider SP, Mahajan A, Zeevi T, et al. PET/CT radiomics signature of human papilloma virus association in oropharyngeal squamous cell carcinoma. *Eur J Nucl Med Mol Imaging.* 2020;47:2978-2991.

5. Fedorov A, Beichel R, Kalpathy-Cramer J, et al. 3D Slicer as an image computing platform for the Quantitative Imaging Network. *Magn Reson Imaging.* 2012;30:1323-1341.

6. Pyradiomics-community. Pyradiomics Documentation Release v3.0.1. https://pyradiomics.readthedocs.io/_/downloads/en/v3.0.1/pdf/. Accessed June 6th, 2022.

7. Leijenaar RT, Nalbantov G, Carvalho S, et al. The effect of SUV discretization in quantitative FDG-PET Radiomics: the need for standardized methodology in tumor texture analysis. *Sci Rep.* 2015;5:11075.

8. van Griethuysen JJM, Fedorov A, Parmar C, et al. Computational Radiomics System to Decode the Radiographic Phenotype. *Cancer Res.* 2017;77:e104-e107.

9. Chen T, Guestrin C. XGBoost: A Scalable Tree Boosting System. *arXiv e-prints*; 2016.

10. De Jay N, Papillon-Cavanagh S, Olsen C, El-Hachem N, Bontempi G, Haibe-Kains B. mRMRe: an R package for parallelized mRMR ensemble feature selection. *Bioinformatics.* 2013;29:2365-2368.

11. *rBayesianOptimization: Bayesian Optimization of Hyperparameters* [computer program]. Version 1.1.0; 2016.

12. Zwanenburg A, Vallières M, Abdalah MA, et al. The Image Biomarker Standardization Initiative: Standardized Quantitative Radiomics for High-Throughput Image-based Phenotyping. *Radiology.* 2020;295:328-338.

13. Aerts HJ, Velazquez ER, Leijenaar RT, et al. Decoding tumour phenotype by noninvasive imaging using a quantitative radiomics approach. *Nat Commun.* 2014;5:4006.

14. Bouckaert RR, Frank E. Evaluating the Replicability of Significance Tests for Comparing Learning Algorithms. Berlin, Heidelberg: Springer Berlin Heidelberg; 2004:3-12.